FINAL REPORT

SEPTEMBER 1985

TITLE: DESIGN, DEVELOPMENT AND STUDY OF THE CHARACTERISTICS OF TRANSDUCERS FOR THE ULTRASONIC INSPECTION OF OFFSHORE STRUCTURES

DSS FILE NUMBER 21ST. 23440-4-9077

PRINCIPAL INVESTIGATOR: D.A. HUTCHINS

CO-INVESTIGATOR: H.D. MAIR

CONTRACT SERIAL NO: OST84-00139

CONTRACTOR: Queen's University

OCT 14 1986

MICROMEDIA

EXECUTIVE SUMMARY

A study of the characteristics of ultrasonic transducers has been undertaken, involving both theory and experiment. Theoretical computer programs have been developed to predict the pressure variations due to a range of transducers, vibrating at a single frequency. The predictions of theory have been compared to experiment for both PZT and PVDF transducers, and good agreement obtained. This indicates that the work achieved its principal aim of characterizing the outputs of ultrasonic transducers operating in water.

Une étude sur les caractéristiques des transducteurs à ultrasons a été entrepise, impliquant l'aspect théorique et expérimental. Un programme pour ordinateur a été développé pour calculer théoriquement les variations en pression de différents transducteurs, vibrant à une seule fréquence. Pour les transduceurs de PZT et PVDF, les prédictions theoriques ont été composes aus resultats expérimentaux et se sont avenes être en bons accords. Ceci indique que le présent travail a attient son but principal qui etait la caracterisation des rendendements des transducteurs à ultrasons opérant dans l'eau.

INTRODUCTION

An important aspect of all ultrasonic imaging systems is the design of the transducer. In many cases this takes the form of a planar disc vibrating in its so-called thickness-mode, although more advanced designs based on annuli, bowls, cones etc. are in use for specialized applications[1,2]. The resulting pressure fields from disc transducers have received much attention in the literature, and a brief summary of previous work will be presented below. However, it would appear that a rigorous comparison between theory and experiment for harmonically excited disc transducers has been absent to date. In this investigation, the three-dimensional pressure fields in both the nearfield and farfield have been determined experimentally, and compared to theory assuming certain source characteristics.

Some experimental work has been reported on the sampling of radiated pressure fields to a high resolution. Two techniques are popular. The first involves the use of a scanned hydrophone, in the form of either a miniature detector[3] or a thin, metallized membrane[4]. In this approach, resolution is limited by the physical size of the detector, which is difficult to fabricate with diameters less than ~0.5mm. To illustrate the problems that result, consider a 10MHz field in water, where the resultant wavelength λ in water is ~0.15mm. A 0.5mm diameter hydrophone is thus ~3.3λ in cross-section, and much detail will be lost. Such a hydrophone would only be able to sample fields properly at frequencies <~1MHz. It should be noted, however, that a specially-constructed hydrophone of 0.15mm diameter was used by Hayman and Weight[5] to investigate transient waveforms from circular and square tansducers. A second approach is to use a small reflector to sample the field, with the transducer under test being used in a pulse-echo mode. Sachse and Hsu[6] have described the type of results obtainable, but this approach is more indirect and requires

the nature of the transducer as a receiver to be known if a rigorous measurement is to result.

The present authors wished to study the pressure fields of ultrasonic transducers to a resolution of $\lambda/5$, so as to ensure that important details in interference phenomena were observed properly. It was thus decided to use a 1mm diameter scanning hydrophone, with an excitation frequency of ~300kHz. This resulted in λ~5mm in water. While this frequency is lower than that used in typical imaging systems, the experiments to be described may be thought of as a scaled model of transducer behaviour at higher frequencies. For instance, a 5mm radius transducer operating at 1.5MHz would be modelled in our experiment as a similar transducer of 25mm radius excited at 300kHz, to retain the correct ratio of a/λ, a being the transducer radius.

A fundamental aim of the present investigation was to compare experiment to theory. Various theoretical approaches are available for the case of harmonic excitation, and the reader is referred to the work of King[7], Zemanek[8], and Lockwood and Willette[9] for a discussion of the theoretical fields from plane pistons. Further work by Archer-Hall and Gee[10] showed that from geometrical arguments, the field of a plane piston could be expressed in the form of a single integral. This and other approaches have been reviewed by Harris[11], who also treated the case of pulsed excitation.

In all cases to be considered, it is required to find a solution to the surface integral of the form

$$\phi = \iint_S \frac{e^{-jks}}{s} \, ds \qquad (1)$$

where s is the distance of the field point to some element on the surface of the disc, and ϕ is the scalar velocity potential. Note that the time dependence is omitted, as pressure is proportional to the time differential of ϕ, which does not affect amplitude variations in the field. This expression holds for a plane piston vibrator, but other discs in which the amplitude of

vibrations varies across the front face may be investigated, as will be shown later. Previous studies have shown that such variations can have a marked influence on radiated pressure fields. Lockhart and Miller[12] investigated the directivity patterns of transducers, and demonstrated a reduction in side lobe predominance by using a line shading. This effect had been noted earlier by Martin and Breazeale[13] and Papadakis[14]. Theoretically, Szabo[15] predicted the beamshaping and diffraction from tapered amplitude distributions, using theory derived from optics, but the various acoustic parameters were not identified. However, a Gaussian distribution across the face was seen to lead to a uniform radiated beam. Truncated Gaussian profiles were also effective in this respect.

In an extension of the theory for a piston radiator, Greenspan[16] examined the radiated field of a transducer with a Gaussian particle velocity distribution across its face. In agreement with Szabo[15], axial nearfield intensity variations were smoothed out, when a comparison was made to those of a uniform vibrator. Recent advances have been made by both Tjøtta and Tjøtta[17], and Harris[18], who evaluated the transient field of pulsed pistons with nonuniform velocity distributions. The former authors derived expressions to describe the field for several amplitude distributions, whereas Harris presented impulse and pulse response functions for different axisymmetric source velocity distributions and pulse shapes.

The present authors have examined the theory for a plane piston under harmonic excitation, and will show that a single integral expression be derived from first principles. This expression, which is equivalent to that derived by other authors[10] using geometrical arguments, is then used in a modified form to investigate non-uniform radiators for a comparison to experiment, as will now be described.

THEORY

In this section, an expression for the scalar velocity potential $\phi(\rho,z)$ within the field of a plane piston will be derived, as a function of radial (ρ) and axial (z) coordinates. This will be followed by a description of how such an approach may be used to examine non-uniform axisymmetric vibrators.

Assumming an angular frequency $\omega = kc$, where k is a wavenumber and c the acoustic velocity, the velocity potential which satisfies the Helmholtz equation

$$(\nabla^2 + k^2)\phi = 0 \tag{2}$$

may be written as

$$\phi(\underline{r}) = \int_S d\underline{S}'.[G_k(\underline{r},\underline{r}')\ \nabla'\phi(\underline{r}')\ \nabla'\phi(\underline{r}') - \phi(\underline{r}')\nabla'G_k(\underline{r},\underline{r}')] \tag{3}$$

where G_k is a Green function for the Helmholtz equation, and satisfies the following:-

$$(\nabla'^2 + k^2)G_k(\underline{r},\underline{r}') = (\nabla^2 + k^2)G_k(\underline{r},\underline{r}') = -\delta(\underline{r}-\underline{r}') \tag{4}$$

Note that in equations (3) and (4), $\underline{r}$ is a field coordinate and $\underline{r}'$ a coordinate on the z=0 plane, containing the disc face. A boundary condition of the form

$$d\underline{S}'.\nabla'G_k = 0 \text{ when } z' = 0 \tag{5}$$

is to be imposed; a solution of eq. (4) which satisfies this condition may be written as

$$G_k(x,y,z;\ x',y',z') = g_k(x-x',y-y',z+z') + g_k(x-x',y-y',z-z')$$

$$\text{with } g_k(\alpha,\beta,\xi) = \frac{e^{-jk\sqrt{\alpha^2+\beta^2+\xi^2}}}{4\pi\sqrt{\alpha^2+\beta^2+\xi^2}}$$

The above expresses the result in Cartezian coordinates (x,y,z), but it is now convenient to introduce cylindrical coordinates

$$\rho = \sqrt{x^2+y^2}\ , \qquad \gamma = \tan^{-1}(y/x),\ z$$

where ρ is a radial coordinate and γ the azimuthal angle. Equation (3) then reduces to

$$\phi(\underline{r}) = -2\int_o^\infty d\rho'\rho' \int_o^{2\pi} d\gamma.\ g_k(x-x',y-y',z).\ \frac{d\phi}{dz'}(x'y',0)$$

However, boundary conditions dictate that the z component of particle velocity q_z be considered over the transducer face, being zero outside it for the infinite baffle boundary condition. q_z is defined as

$$q_z = \frac{\partial\phi}{\partial z}$$

and if we write q_z across the transducer face as some function of ρ at the $z = 0$ plane, i.e.

$$q_z(\rho,0) = F(\rho)$$

we obtain

$$\phi(\underline{r}) = -2\int_o^\infty \rho'\ F(\rho')\ d\rho' \int_o^{2\pi} g_k(x-x',y-y',z)d\gamma$$

Now in this case,[20]

$$g_k(x-x',y-y',z-z') = \frac{j}{4\pi} \sum_{m=-\infty}^{\infty} e^{jm(\phi-\phi')} \int_o^\infty P.J_m(P_\rho)J_m(P_{\rho'}). \qquad (6)$$

$$. \frac{e^{-j|z-z'|\sqrt{k^2-P^2}}}{j\sqrt{k^2-P^2}} .dP$$

where P is a variable of integration.

The ϕ' integration in eq. (6) eliminates all but the m=0 term, so that eq. (6) becomes

$$\phi(\rho,z) = -\int_o^\infty d\rho'\ \rho' F(\rho') \int_o^\infty dP.PJ_o(P\rho)J_o(P\rho').$$

$$. \frac{e^{-jz\sqrt{k^2-P^2}}}{j\sqrt{k^2-P^2}} \qquad (7)$$

For a plane piston, the particle velocity is a constant (U) over the disc radius a, and zero elsewhere i.e.

$$F(\rho') = \begin{cases} U, & o<\rho'<a \\ o, & \rho'>a \end{cases}$$

Thus the ρ' integration becomes

$$U\int_o^a d\rho'\ \rho'\ J_o(P\rho') = \frac{1}{P^2} \int_o^{Pa} d(P\rho').\ P\rho'.J_o(P\rho')$$

$$= \frac{Ua}{P} J_1(Pa)$$

and

$$\phi(\rho,z) = -Ua \int_o^\infty J_o(P\rho)J_1(Pa) \frac{e^{-jz\sqrt{k^2-P^2}}}{j\sqrt{k^2-P^2}} .dP \qquad (8)$$

However, the Bessel function terms may be expressed as

$$J_o(P\rho)J_1(Pa) = \frac{1}{2\pi} \int_{-\pi}^{\pi} J_1\left(\frac{P\sqrt{\rho^2+a^2-2a\rho\cos\psi}}{(\rho^2+a^2-2a\rho\cos\psi)^{1/2}}\right)(a-\rho e^{-j\psi})d\psi$$

where ψ is a variable of integration.

Introducing this integral representation into eq. (8), and using Hankel Transform tables , leads to

$$\phi(\rho,z) = -\frac{Uaj}{2\pi k} \int_{-\pi}^{\pi} \left(e^{-jk\sqrt{R^2+z^2}} - e^{-jkz}\right) . \left[\frac{a-\rho e^{-j\psi}}{R^2}\right] d\psi \qquad (9a)$$

where again ψ is a variable of integration, and R is given by

$$R^2 = \rho^2 + a^2 - 2a\rho\cos\psi = (a-\rho e^{-j\psi})(a-\rho e^{j\psi}) \qquad (9b)$$

Equations (9) are the required expressions to allow the scalar velocity potential $\phi(\rho,z)$ to be evaluated at any point in the radiation field. Equation (9) is, in fact, equivalent to that derived by Arthur-Hall and Gee[10] by geometrical arguments. To illustrate this let $S^2 = R^2 + z^2$, where S is the distance from a surface element to the field point. Splitting up the integral, we obtain two parts. The first is

$$\int_{-\pi}^{\pi} e^{-jks}\left(\frac{a-\rho e^{-j\psi}}{R^2}\right)d\psi \qquad (10)$$

whereas the second integral becomes

$$-e^{-jkz}\int_{-\pi}^{\pi}\frac{a-\rho e^{-j\psi}}{R^2}\,d\psi = -e^{-jkz}\int_{-\pi}^{\pi}\frac{d\psi}{(a-\rho e^{j\psi})} \qquad (11)$$

The second integral, eq. (11), may be solved by a contour method or from integral tables. The result is

$$-e^{-jkz}\,\frac{2\pi}{a}\cdot\begin{bmatrix} 1 & \rho < a \\ 1/2 & \rho = a \\ 0 & \rho > a \end{bmatrix} \qquad (12)$$

and hence this term is $e^{-jkz}\,\frac{2\pi}{a}$ for radial distances less than the transducer radius a, half that value when $\rho = a$ and zero at greater distances. The first part (eq. (10)) is, by symmetry,

$$\int_{-\pi}^{\pi} e^{-jks}\,\frac{(a-\rho\cos\psi z)}{R^2}\,d\psi = 2\int_{o}^{\pi} e^{-jks}\,\frac{(a-\rho\cos\psi)}{R^2}\,d\psi$$

Hence eq. (9) becomes

$$\phi(\rho,z) = -\frac{Uaj}{2\pi k}\left\{-\frac{2\pi}{a}\begin{bmatrix} 1 \\ 1/2 \\ o \end{bmatrix} e^{-jkz} + 2\int_{o}^{\pi} e^{-jks}\,\frac{(a-\rho\cos\psi)}{R^2}\,d\psi\right\}$$

$$= \frac{Uj}{k}\begin{bmatrix} 1 \\ 1/2 \\ o \end{bmatrix} e^{-jkz} + \frac{Uaj}{\pi k}\int_{o}^{\pi} e^{-jks}\left(\frac{\rho\cos\psi-a}{R^2}\right)d\psi \qquad (13)$$

Omitting an arbitrary constant, $\frac{Uj}{k}$, and multiplying through by a within the

integral, we obtain the result

$$\phi(\rho,z) = \begin{bmatrix} 1 \\ 1/2 \\ 0 \end{bmatrix} e^{-jkz} + \frac{1}{\pi}\int_0^{\pi} e^{-jks}\,\frac{(a\rho\cos\psi - a^2)}{(a^2+\rho^2-2a\rho\cos\psi)}\,d\psi \qquad (14)$$

which is the result derived by Archer-Hall and Gee.[10]

The above result (equations (9) and (14)) leads to the evaluation of the scalar velocity potential for a single plane piston. Note, however, that at a single harmonic frequency ω, the acoustic pressure P_a at a point within the radiated field is given by

$$\begin{aligned} P_a &= -\rho d\phi(\rho,z)/dt \\ &= -j\omega\rho\phi(\rho,z) \end{aligned}$$

Hence, relative variations in acoustic pressure are equivalent to those of scalar velocity potential.

In the above, the amplitude U of particle velocity across the disc face is constant. Consider, however, the case where this value changes in both amplitude and phase with radius. In the results that follow, this phenomenon will be examined experimentally. Theoretically, however, such an effect may be considered by the addition or subtraction of several plane piston contributions.

As an example, the field from an annulus (or "ring" transducer) may be simply described by the subtraction of the field of one disc from another of similar amplitude but larger radius. This is illustrated in Fig. 1(a). Similarily, an increased number of plane piston radiators can be used to describe more complicated situations. For example, Fig. 1(b) demonstrates how a decrease in amplitude with radius across a single disc may be synthesized by the addition of successive plane pistons of varying radius. In this example, U is the same for all plane piston contributions.

Changes in phase across the disc may also be modelled, by considering U to be complex i.e. with an amplitude and phase component. Hence, in a similar fashion to real amplitude above, the phase may be altered with radius

(ρ) by the superposition of the fields from a number of plane pistons, whose phases are adjusted appropriately.

As an example of the above approach, the fields predicted from a plane piston and a gaussian radiator (i.e. one in which U decreases as a gaussian with radius) are presented in Figs. 2 and 3 respectively for a frequency such that $a=5\lambda$. In these figures, (a) is the axial pressure field, (b) is the field as a three-dimensional graph, plotted to an axial distance z of 6a, and (c) is a contour representation. Note the marked differences in the two fields. The plane piston exhibits the well-known maxima and zeroes on-axis, with large changes in pressure amplitude within the nearfield and a tendency for side-lobe production. These phenomena agree with those published previously.[8-11] The gaussian radiator exhibits a smooth axial field, as noted earlier by Greenspan[16]; the three dimensional field shows in greater detail how this uniformity is a feature of the whole field, with side-lobes being absent. A comparison of the contour plots for these two types of radiator (Figs. 2(c) and 3(c) respectively) reinforces the differences between the two.

Theoretically, any variations in amplitude and phase across the face of a disc may be modelled, provided cylindrical symmetry exists. To investigate these effects experimentally, an apparatus designed to study radiated fields of disc transducers to a high resolution has been constructed as will now be described.

APPARATUS

To study transducer fields to a high resolution, it was decided to use an experimental frequency of ~300 kHz, where the radiated wavelength λ in water was ~5mm. The use of a 1mm diameter hydrophone then led to a measurement resolution of ~$\lambda/5$, deemed suitable for a comparison to theoretical predictions. The transducers used were fabricated from either PZT (lead zirconate titanate), a piezoelectric ceramic, or PVDF (polyvinylidence fluoride), a piezoelectric polymer, usually with a radius (a) of 25.4mm. Thus, with excitation at ~300kHz, these transducers operated under the condition $a \approx 5\lambda$.

The two types of transducer were mounted through one wall of a water tank in specialized holders. PZT transducers were mounted simply in an aluminum holder, using silicon rubber cement as a waterproofing agent (Fig. 4(a)). PVDF transducers were fabricated by cementing the PVDF film, usually of 90μm thickness, to an aluminum backing plate, using epoxy under pressure to obtain a smooth, wrinkle-free finish. This arrangement is shown schematically in Fig. 4(b). Great care was taken to ensure that these holders resulted in the transducer face being flush with the water tank wall, to simulate infinite baffle conditions.

The complete apparatus is shown schematically in Fig. 5. The radiated field was sampled by a scanning hydrophone, fabricated from a 1mm diameter, 2MHz PZT element damped by an epoxy backing. Note that this frequency was well above that of 300kHz, and resonance of the hydrophone was not observed to distort waveforms unduly. The hydrophone was scanned under computer control, using a 1mm pitch threaded drive and automatic backlash compensation ,achieved by always stopping the motors under drive in the same direction under hardware control.

For example, in the negative direction along a particular axis, the motors executed 20 additional steps, stopped, and then returned 20 steps in the positive direction to arrive at the correct position.

The same computer (Apple IIe) controlled data collection using a 12 bit A/D converter, which sampled the d.c. output from a gated peak detector with an adjustable gate delay and width. This voltage was proportional to the peak pressure detected by the hydrophone. To simulate continuous-wave emission, a 30V

tone burst (~50 cycles typically) at 300 kHz was used as the voltage excitation, with the gate delay set so as to sample only that portion of the emitted transient over which the amplitude was constant. In this way, transients at the beginning and end of the signal, plus side wall reflections, were not sampled, the result being an excellent simulation of continuous-wave emission.

The digitized data was transferred to disc for storage at the end of each single scan of the hydrophone, which could be moved in any of three orthogonal directions. In the cases to be presented here, the scans were undertaken as a series of single sweeps horizontally across the transducer (i.e. in the ρ direction), at various distances z from the transducer. A typical measurement would be performed over a 100mm radial and 300mm axial distance, in the form of 61 scans separated by 5mm. It should be noted that the ultimate resolution of the stepping motor drive system was 5μm.

EXPERIMENTAL RESULTS AND COMPARISON TO THEORY

Various PZT and PVDF transducers have been investigated using the above apparatus, and the results are presented below. In the case of PZT transducers an additional measurement was required to ascertain its vibrational characteristics, as will be described. The two types of transducer are now considered separately.

A. PVDF transducers

The mounting arrangement of these transducers was shown schmatically in Fig. (4b). An aluminum backing was chosen, as it maximized damping and increased the efficiency of generation, while supplying the required rigidity. This type of mounting has, in fact, been used successfully by other workers in the medical field for cone transducers.[2] Other mounting techniques were attempted, but an aluminum backing performed better than a polymer variety which attempted to match impedances. Note that the high resonant frequency of the PVDF (~16MHz for 90μm material) ensured that little distortion of 300kHz signals occured. Using such a mounting technique, it might be expected that the PVDF might act like a plane piston i.e. there would be no obvious mechanisms (such as radial modes) that would cause the vibrational amplitude or phase to vary with radius.

The first PVDF transducer investigated was a planar disc of 25mm radius, vibrating at 300kHz, the measured pressure field being shown in Fig. 6. Note marked variations in amplitude within the nearfield region, a tendancy for side lobe predominance and a high degree of axial symmetry, all expected if the transducer was behaving as a plane piston radiator (Fig. 2(b)). The measured axial field is presented in Fig. 6(b), the corresponding theoretical field being shown previously in Fig. 2(a). Note that while the maxima and minima are in the expected positions, the minima in the experimental field were not zeroes. This was expected, as it has been found in practice that even small changes in the edge geometry of the PVDF led to significant changes in the

axial field. It would thus be very difficult to obtain zeroes in practice, as these require perfect destructive interference which is very sensitive to edge effects.

To facilitate the comparison further, the experimental and theoretical fields are replotted in the same format and presented together in Fig. 7. It is clear from Figs. 7 and 6 that the PVDF disc was exhibiting plane piston-like behaviour.

As a further test of the above, and to examine the theoretical approach for non-uniform vibrators, two annuli of differing dimensions were fabricated from PVDF and again attached rigidly to an aluminum backing. The first was of outside radius 25mm and radial thickness 5mm, excited at a frequency of 300kHz. The experimental and theoretical fields for such a transducer are compared in Fig. 8, where the theoretical approach follows the subtraction technique outlined earlier in Fig. 1(a). Reasonable agreement is observed, with the presence of a single axial maximum and a series of prominent side lobes in both theory and experiment.

A second annulus of larger radial thickness was also fabricated, with an outside diameter of 50mm and a effective radial thickness of 25mm, excited at a frequency of 400kHz. Theory and experiment are compared in Fig. 9 for this case, for both the three-dimensional and axial pressure fields respectively. Again, good agreement existed between theory and experiment. Note now that more than one axial maximum was present, and that the field was more akin to that expected from a plane piston.

B. PZT transducers

These transducers were fabricated using PZT-4 ceramic from Almax Industries Ltd., and the first series of experiments were undertaken with 25.4mm radius discs of 300kHz nominal resonant frequency. They were mounted as shown in Fig. 4(a), with an air backing initially. In such a configuration, a series of frequencies were found at which efficient ultrasonic radiation ensued, and the resulted fields determined experimentally are presented in Fig. 10 at (a) 293kHz, (b) 300kHz and (c) 304.2kHz.

The fields of Fig. 10 show interesting features. At a frequency of 293kHz, a prominent pressure peak was observed on-axis, at a distance of 10mm (i.e. at $z \approx 2\lambda$) from the transducer face. The nominal nearfield/farfield boundary, as judged by the position of the last axial maximum, was at 12.5cm ($\sim 25\lambda$), close to that expected from simple considerations (i.e. assuming a plane piston). The overall pressure field, however, was markedly different from that expected from a plane piston, Fig. 2, in that there was poor farfield radiation in the main lobe, a higher level of side lobes and the large pressure peak on-axis mentioned above. At 300kHz, Fig. 10(b), the radiated field was somewhat different being more uniform. The axial response still contained oscillations in amplitude, but these were less marked than at 293kHz, with the prominent pressure peak of Fig. 10(a) being less prominent. In addition side lobe levels were reduced, with the result that the beam was more directional. Finally, at 304.2kHz (Fig. 10(c)), the field seemed again to be more uniform and directional than at lower frequencies, a prominent peak in pressure on-axis at a small distance from the transducer face being absent. Note that in Figs. 10(b) and (c), the last axial maximum was not at the expected position for a plane piston radiator.

To understand the effects that might cause a prominent axial pressure maximum to be present, consider the field that would be radiated theroetically

by a disc whose amplitude of vibration varies markedly with radius. In Fig. 11, the field of a disc is presented whose amplitude exhibits several maxima and minima (four cycles of a cosine function) across its radius. Note that a prominent axial pressure maximum is predicted, as observed experimentally. Hence, it was concluded by the authors that radial modes of PZT discs were causing variations in amplitude of vibration with radius, leading to a large constructive interference peak in the experimental field plots.

To investigate the above effects further, an additional experiment was conducted, with a PZT disc removed from the water tank. A capacitance transducer was used to sample the displacement d at various positions across the disc diameter. The capacitance transducer was of a ball-bearing design, and is shown schematically in Fig. 12. The PZT disc was scanned horizontally using translation stages, and at each sampling position the ball-bearing wound down close to surface by a micrometer, with a thin (~25μm) polymer spacing sheet to both keep the capacitance constant and to increase the dielectric constant in the gap (and hence the sensitivity). At 297kHz, the disc was observed to have marked displacement variations across its face, as shown in Fig. 13. The phase at each point was always measured, but varied little across the disc radius, except at the nodes where changes in phase would have little effect on the resultant pressure field.

Note, that both amplitude and phase were measured using a Solartron 1170 Frequency Response Analyzer.

Using the approach outlined in the previous Theory Section, it was possible to predict theoretically the radiated pressure field of a disc whose amplitude changed with radius as in Fig. 13. The result is presented in Fig. 14, and a comparison to experiment demonstrates that the principal features of the experimental field are predicted i.e. the prominent axial pressure peak and the poor farfield radiation characteristics. It should be noted that the above is not a rigorous comparison because of the different loading characteristics of water and air. However, the results indicate that cross-coupling to radial modes is the primary factor influencing the radiated

fields of the resonant PZT discs examined, due to a non-uniform displacement (and hence velocity U_z) distribution across their front face.

Note that the distribution of Fig. 12 is not exactly symmetrical, and the average across a radius was taken theoretically. This might explain the slight differences observed between theoretical predictions and experiment

As the features shown in Figs. 10(a) and (14) are undesirable for such applications as acoustical imaging, it is important that these radial modes be suppressed. One approach is to use a different piezoelectric material such as PVDF, where the radial modes may be negligible. If, however, PZT is the required material, then remedial measures must be taken.

A traditional approach is to back the PZT disc with a damping material such as tungsten/epoxy mixtures. This is under active study by the authors at present. Initial results with the PZT discs used in the present paper is that the effect seems to be marginal. This might be expected for the discs used, which are of a low frequency and hence fairly thick (7mm). Backings would be expected to have a much greater effect on thinner discs (e.g. the disc used at 3MHz, typical in many applications such as medical imaging and nondestructive testing, would be one tenth as thick), and this will be studied as further work. It has also been suggested that a central hole through the disc would tend to discourage certain radial modes. This has been observed by the authors to have an effect in some cases, but not in others. It would seem to depend strongly on geometry, and again will be studied as further work.

FURTHER PREDICTIONS OF THEORY

As outlined in the Theory Section, an approach for the fields of disc transducers has been developed which can consider variations in amplitude and phase across the front face of axisymmetric transducers. In view of the fact that pressure fields of disc radiators with a variety of vibrational characteristics do not seem to have been published extensively, we thought it instructive to present several further examples of the technique.

Figs. 2 and 3 showed the field from a plane piston and gaussian radiator respectively, when the frequency of excitation was such that $a=5\lambda$. Consider, for comparison, the case where the vibrational amplitude decreases linearly with radius, the resultant field being shown in Fig. 15(a). The axial field is fairly smooth, and side lobe predominance is low; hence, the linear decrease case shows many features in common with the Gaussian case (Fig. 3). In general the authors have observed that a decrease in vibrational amplitude with radius leads to an increased uniformity of the radiated fields. This is demonstrated further in Fig. 15(b), where the vibrational amplitude is constant between $0<\rho<4a/5$, and thereafter decreases linearly to zero. Even in this case, noticable improvements in uniformity over the plane piston case (Fig. 2) are evident.

In contrast to the above, a linear <u>increase</u> in vibrational amplitude with radius leads to a field characterized by marked nearfield pressure variations and a high level of side lobes. This case is presented in Fig. 15(c)

In most theoretical fields presented above, the phase was considered to be constant across the disc face. However, if the phase varies with radius, the resultant fields will change. This is illustrated by considering a disc transducer, synthesized by 20 concentric annuli around a central disc, such that the phase is different on each zone. These zones were of equal width, and had the same amplitude of vibration. Using such an arrangement, the phases required to focus the pressure field at certain positions on-axis were

determined, the phases input to the theoretical program and the resultant fields plotted in three dimensions. Assuming a 50mm diameter disc radiator (i.e. a=25mm with again a=5λ), the resultant pressure fields are presented in Fig. 16 for foci at (a) 2cm, (b) 5cm and (c) 10cm. Note that the nearfield for a plane piston would extend to a distance of ~12.5cm. As will be noticed in Fig. 16, the accuracy of positioning of the axial focus decreases as the intended focal position moves towards the nearfield/farfield boundary. This would be expected, as this technique would not be applicable to the farfield of the pressure distribution (i.e. Fresnel diffraction no longer applies).

A final field of interest was that due to a zone plate, used extensively in Fresnel focusing.[21] We have investigated the radiated field of such a transducer, using the amplitude distribution shown in in Fig. 17(a). The predicted field is shown in Fig. 17(b) and demonstrates the expected tendancy for an axial pressure maximum within the nearfield. Note that the intended focal point was 20mm from the transducer's front face, a result that agrees well with the theoretical three-dimensional distribution.

OTHER STUDIES AND RECOMMENDATIONS FOR FURTHER WORK

It has been demonstrated that theoretical approaches may be used to predict experimental fields, provided the characteristics of the transducer are known. We have shown that the properties of PVDF transducers make them attractive for certain applications, in that they can be constructed to vibrate in known fashion, i.e. as plane piston radiators. This work was extended to investigate apodizing, where known variations in voltage amplitude could be applied to concentric annuli of PVDF. Unfortunately, it was found that the fabricated procedure, involving attachment to an aluminum backing, was not reproducible. Hence, each annulus did not vibrate with the same amplitude when similar voltage were applied. At present, we are investigating whether a correction procedure may be adopted. However, a more promising route may be the use of composite materials, with small PZT elements embedded in a polymer matrix. It is planned to investigate such an approach as future work.

An important aspect of underwater transducer design is the prediction of the complete pressure field from a single measurement in the nearfield. In this regard, it was planned to use the approximate series approach of Guyomar[22]. However, it would appear to the authors that this method is only applicable to a certain range of transducer parameters. We have not been able to achieve reproducible results at practical transducer dimensions. Presently, a new approach is being developed, which involves measuring the axial field, and subsequently inverting the data to predict the transducer behaviour. Results from this type of approach show promise, and will be investigated further.

CONCLUSIONS

It has been demonstrated that good correlation between experimental and theoretical pressure fields of disc transducers is possible, assuming excitation at a single frequency. Both PVDF and PZT transducers have been investigated in this regard. It was found that PVDF transducers, when fabricated with care, could act as plane piston radiators to a good approximation. PZT transducers, however, were more complicated, in that variations in amplitude across their front face led to marked deviations from plane piston-like behaviour. These phenomena were also a function of frequency. Such conclusions were drawn by the comparison of experimental data to theory, the latter being specially developed to consider variations in amplitude and phase across the transducer face. In addition, various predictions of the theory were presented, of potential interest to workers in acoustical imaging.

ACKNOWLEDGEMENTS

The authors wish to thank the Department of Energy, Mines and Resources and the Advisory Research Committee of Queen's University for financial Support. Additional thanks are given to Dr. Mak and M. Stott for encouragement.

REFERENCES

1. P. Munro, R.P. Hill and J.W. Hunt, Med. Phys. 9, 888-897 (1982).
2. F.S. Foster, M.S. Patterson, M. Arditi and J.W. Hunt, Ultrasound Imaging 3, 62-82 (1981).
3. P.A. Lewin, Ultrasonics 19, 213-216 (1981).
4. R.S. Mezrich, K.F. Etzold and D.H.R. Vilkomerson, R.C.A. Review 35, 483-519 (1974).
5. A.J. Heyman and J.P. Weight, J. Acoust. Soc. Am. 66, 945-951 (1979).
6. W. Sachse and N.N. Hsu, In "Physical Acoustics" Vol. X1V (Academic Press, N.Y., 1979, W.P. Mason and R.N. Thurston eds), pp. 277-406.
7. L.V. King, Can. J. Res. 11, 135-155 (1934).
8. J. Zemanek, J. Acoust. Soc. Am. 49, 181-191 (1970).
9. J.C. Lockwood and J.G. Willette, J. Acoust. Soc. Am. 53, 735-741 (1973).
10. J.A. Archer-Hall and D. Gee, NDT Int. 13, 95-101 (1980).
11. G.R. Harris, J. Acoust. Soc. Am. 70, 10-20 (1981).
12. C.M. Lockhart and M.K. Miller, J. Acoust. Soc. Am. 68, 1142-1148 (1980).
13. F.D. Martin and M.A. Breazeale, J. Acoust. Soc. Am. 49, 1668-1669 (1971).
14. E.P. Papadakis, J. Acoust. Soc. Am. 49, 166-168 (1971).
15. T.L. Szabo, Proc. 1975 IEEE Ultrasonics Symp. 116-119 (1975).
16. M. Greenspan, J. Acoust. Soc. Am. 65, 608-621 (1979).
17. J.N. Tjøtta, and S. Tjøtta, J. Acoust. Soc. Am. 71, 824-833 (1982).
18. G.R. Harris, J. Acoust. Soc. Am. 70, 186-204 (1981).
19. P.M. Morse and H. Feshback "Methods of Theoretical Physics" (McGraw-Hill, 1953), p. 806.
20. Ibid, p. 888
21. B. Noorbehesht, M. Mortezaie, G. Wade and C. Schueler, In "Acoustical Imaging", Vol. X1 (J.P. Powers ed, Plenum Press, N.Y., 1982), pp. 463-478.

22. D. Guyomar, M. Fink and R. H. Coursant, Proc. 1983 IEEE Ultrasonics Symp, 766-769 (1983).

FIGURE CAPTIONS

Fig. 1 Schematic diagram, illustrating how non-uniform vibrational characteristics may be represented as combinations of plane piston contributions.
(a) an annulus, subtraction of one plane piston field from another.
(b) a decrease in amplitude with radius, synthesized by the addition of plane piston fields.

Fig. 2. Theoretical pressure field variations of a plane piston, showing (a) the axial distribution, (b) the field in three dimensions and (c) a contour representation. The disc vibrated such that $a=5\lambda$, where a is the transducer radius and λ the radiated wavelength.

Fig. 3 Theoretical pressure field of a gaussian disc radiator, with $a=5\lambda$. (a) axial distribution, (b) field in three dimensions, (c) contour representation.

Fig. 4 Mounting arrangement of (a) PZT and (b) PVDF transducers, to simulate infinite baffle boundary conditions.

Fig. 5 Schematic diagram of apparatus for the determination of transducer pressure fields.

Fig. 6 Experimental pressure field of a PVDF disc transducer of 25mm radius, excited at 300kHz
(a) three dimensional distribution, (b) axial variation.

Fig. 7 Direct comparison of theory (Fig. 2(b)) and experiment (Fig. 6(a)) for the case of a plane piston.

Fig. 8. Comparison of(a) theoretical and (b) experimental pressure fields for an annulus of outside radius 25mm and width 5mm. Theory assumed a uniform amplitude and phase over the face of the annulus, the experimental transducer being fabricated from PVDF. Frequency of excitation was 300kHz.

Fig. 9 Comparison of (a) theory and (b) experiment for a PVDF annulus, of outside diameter 50mm and width 25mm. Frequency of excitation was

400kHz.

Fig. 10 Experimental pressure fields in water of a 50.8mm diameter PZT disc, excited at (a) λ 293 kHz, (b) 300 kHz and (c) 304.2 kHz. Note axial symmetry in each of the fields.

Fig. 11 Theoretical pressure field of disc, vibrating such that $a=5\lambda$, whose amplitude of particle velocity U_z varied as four cycles of a cosine function across its radius. (a) axial field, (b) three-dimensional distribution.

Fig. 12 Schematic diagram of ball-bearing type capacitance transducer, used to sample the displacements U_z normal to the transducer face.

Fig. 13 The amplitude of displacements across the diameter of a 50.8mm disc, excited in air at 297 kHz.

Fig. 14 (a) The pressure field predicted theoretically for a disc whose face is assumed to vibrate with the amplitude and phase variations of Fig. 13, compared directly to the experimental field at 293kHz (b).

Fig. 15 Theoretical presure fields of discs whose amplitude of vibration U_z varies with radius (a) a linear decrease to zero at the disc edge; (b) constant amplitude over $0<\rho<4a/5$, and a linear decrease to zero at the disc edge thereafter; (c) a linear increase from zero at the disc edge to a maximum at its centre. $a=5\lambda$ throughout. Upper trace of each is the axial field, lower trace the three dimensional distribution.

Fig. 16 Theoretical pressure fields of a disc radiator fabricated from two concentric annuli, surrounding a central disc. The phase of each component was constant across its width, but adjusted so that focusing would be expected to occur at (a) 2cm, (b) 5cm and (c) 10cm from the disc. Upper trace of each is the axial field, lower the three-dimensional distribution. a=25mm, disc vibrated at 300 kHz ($a=5\lambda$ in water).

Fig. 17 Predicted theoretical field (b) of a Fresnel zone plate transducer, whose zones are as shown in (a). For excitation such that $a=5\lambda$, the expected focus would be on axis, at 20mm from the disc face of diameter 5cm.

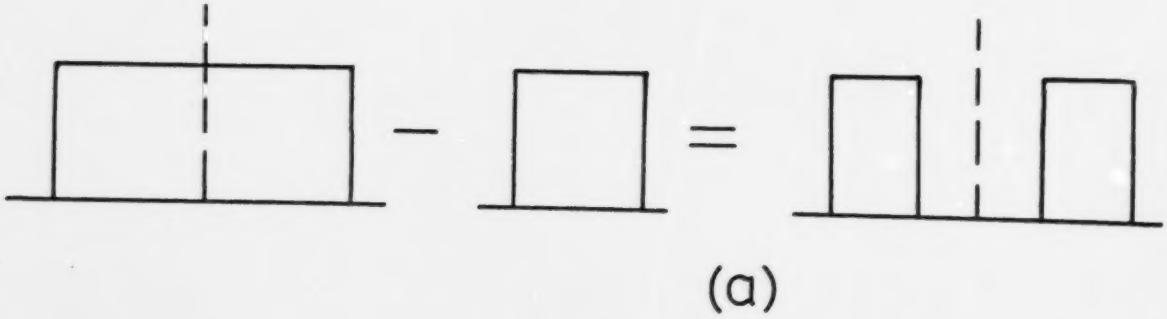

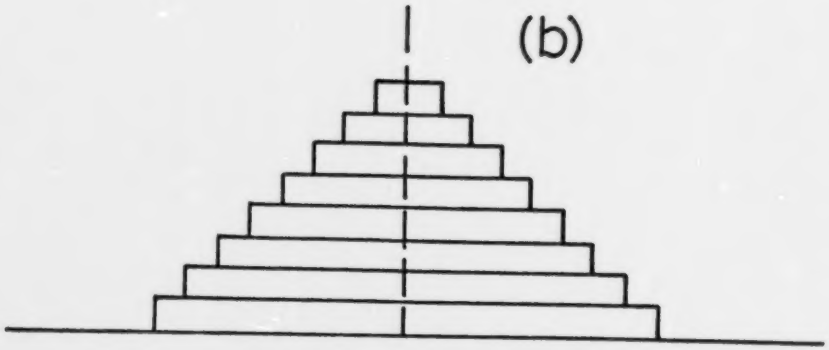

Fig. 1 Schematic diagram, illustrating how non-uniform vibrational characteristics may be represented as combinations of plane piston contributions.

(a) an annulus, subtraction of one plane piston field from another.

(b) a decrease in amplitude with radius, synthesized by the addition of plane piston fields.

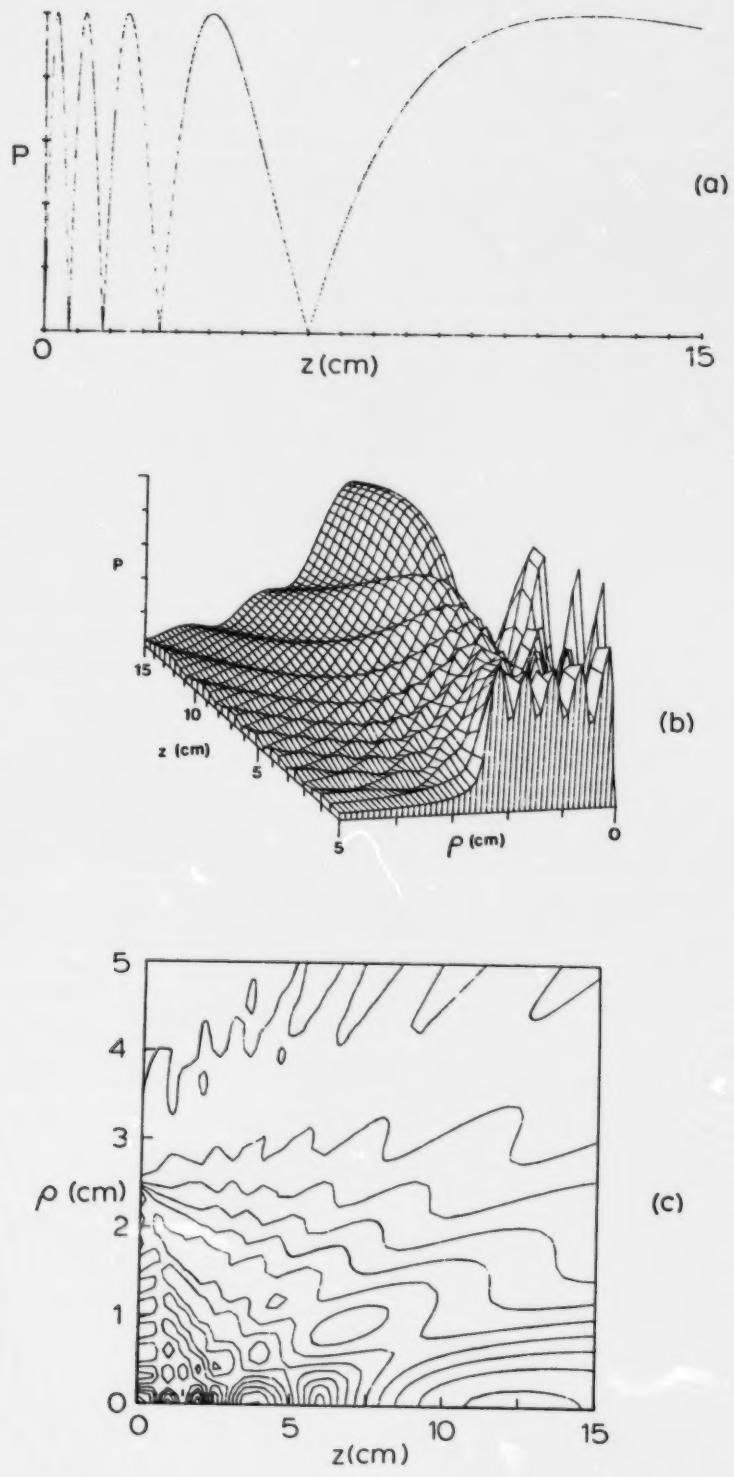

Fig. 2. Theoretical pressure field variations of a plane piston, showing (a) the axial distribution, (b) the field in three dimensions and (c) a contour representation. The disc vibrated such that $a=5\lambda$, where a is the transducer radius and λ the radiated wavelength.

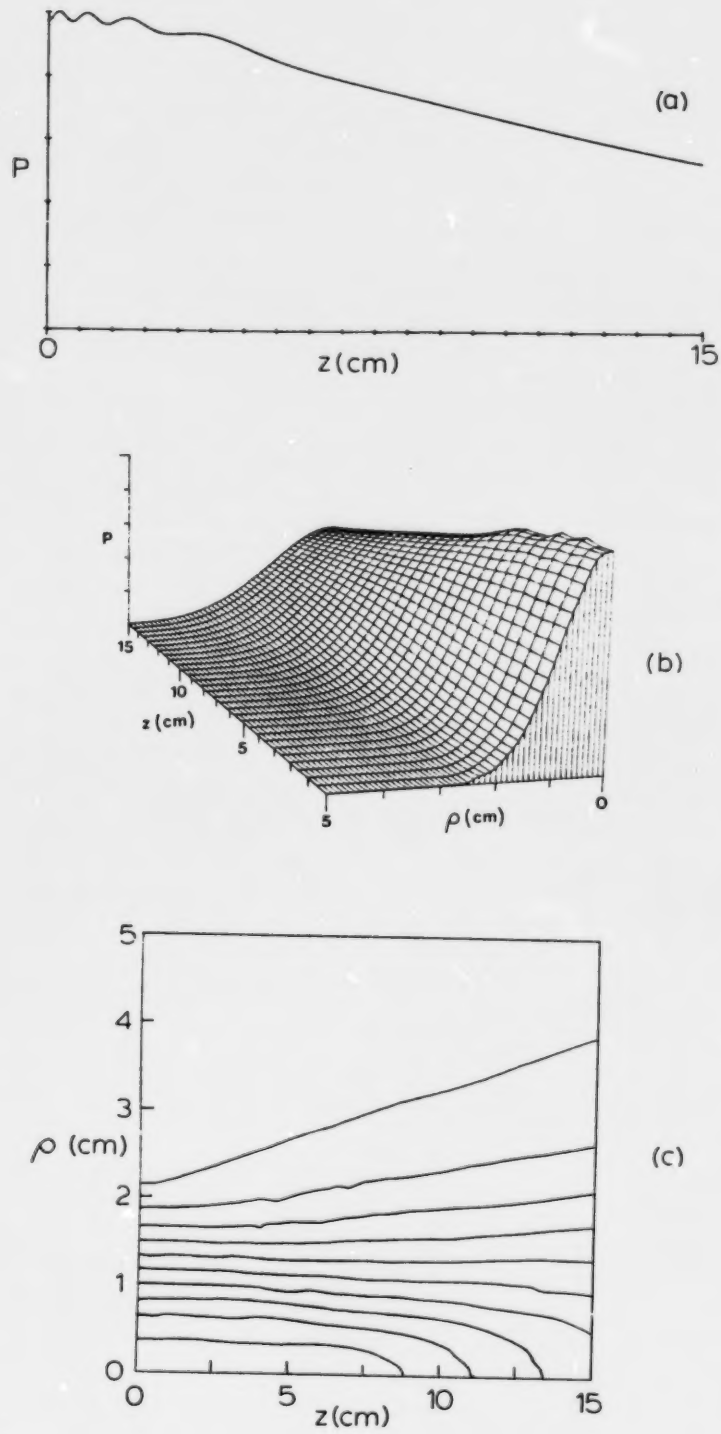

Fig. 3 Theoretical pressure field of a gaussian disc radiator, with a=5λ. (a) axial distribution, (b) field in three dimensions, (c) contour representation.

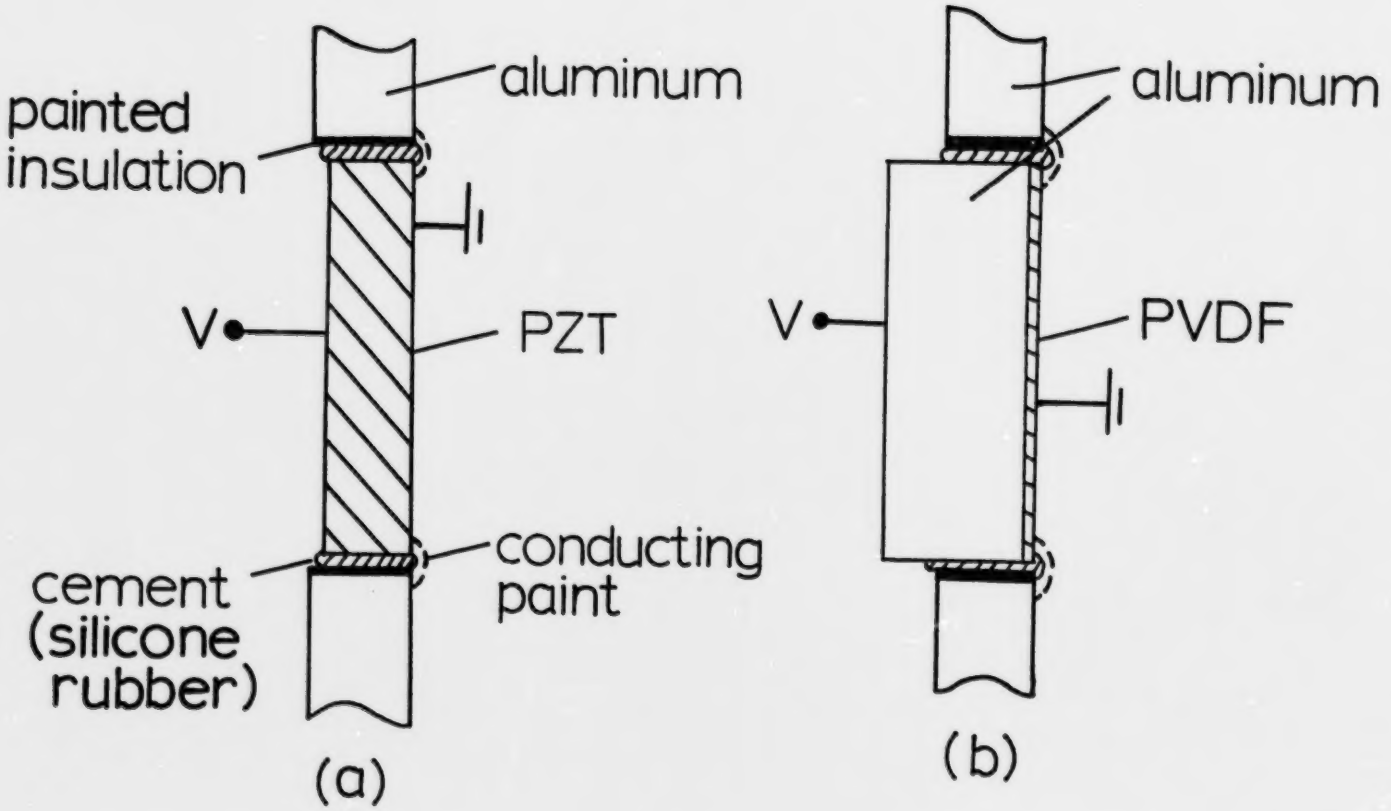

Fig. 4 Mounting arrangement of (a) PZT and (b) PVDF transducers, to simulate infinite baffle boundary conditions.

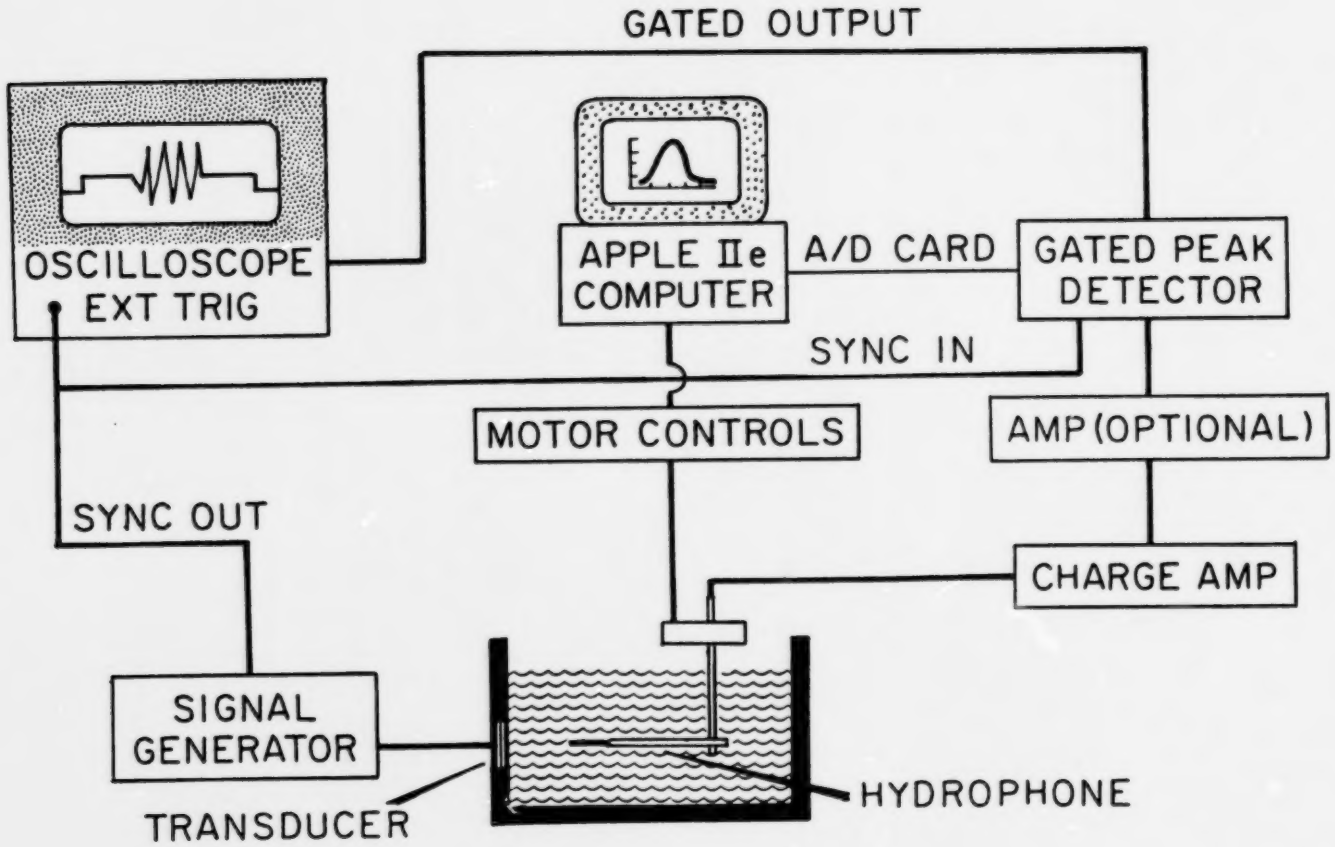

Fig. 5 Schematic diagram of apparatus for the determination of transducer pressure fields.

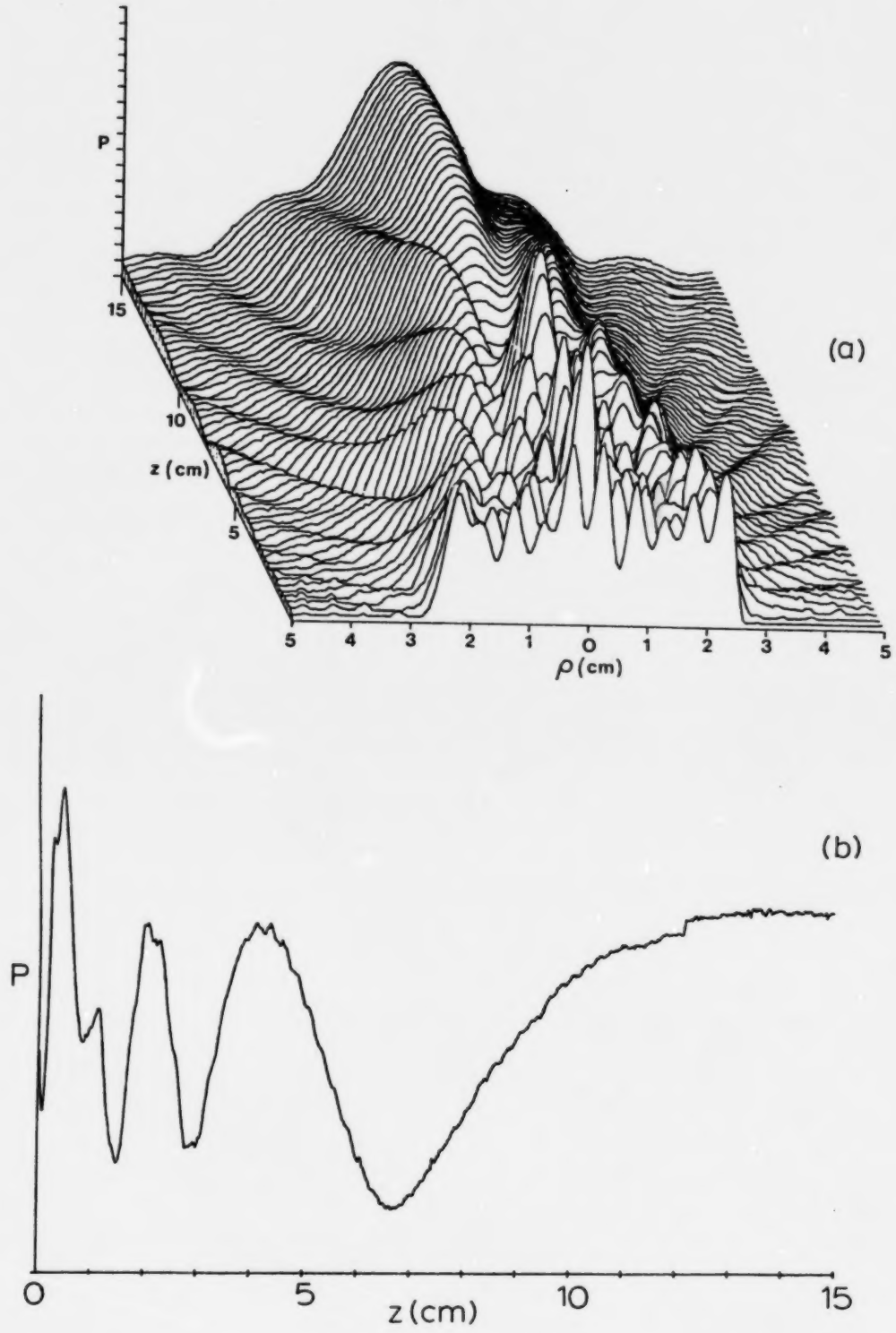

Fig. 6 Experimental pressure field of a PVDF disc transducer of 25mm radius, excited at 300kHz

(a) three dimensional distribution, (b) axial variation.

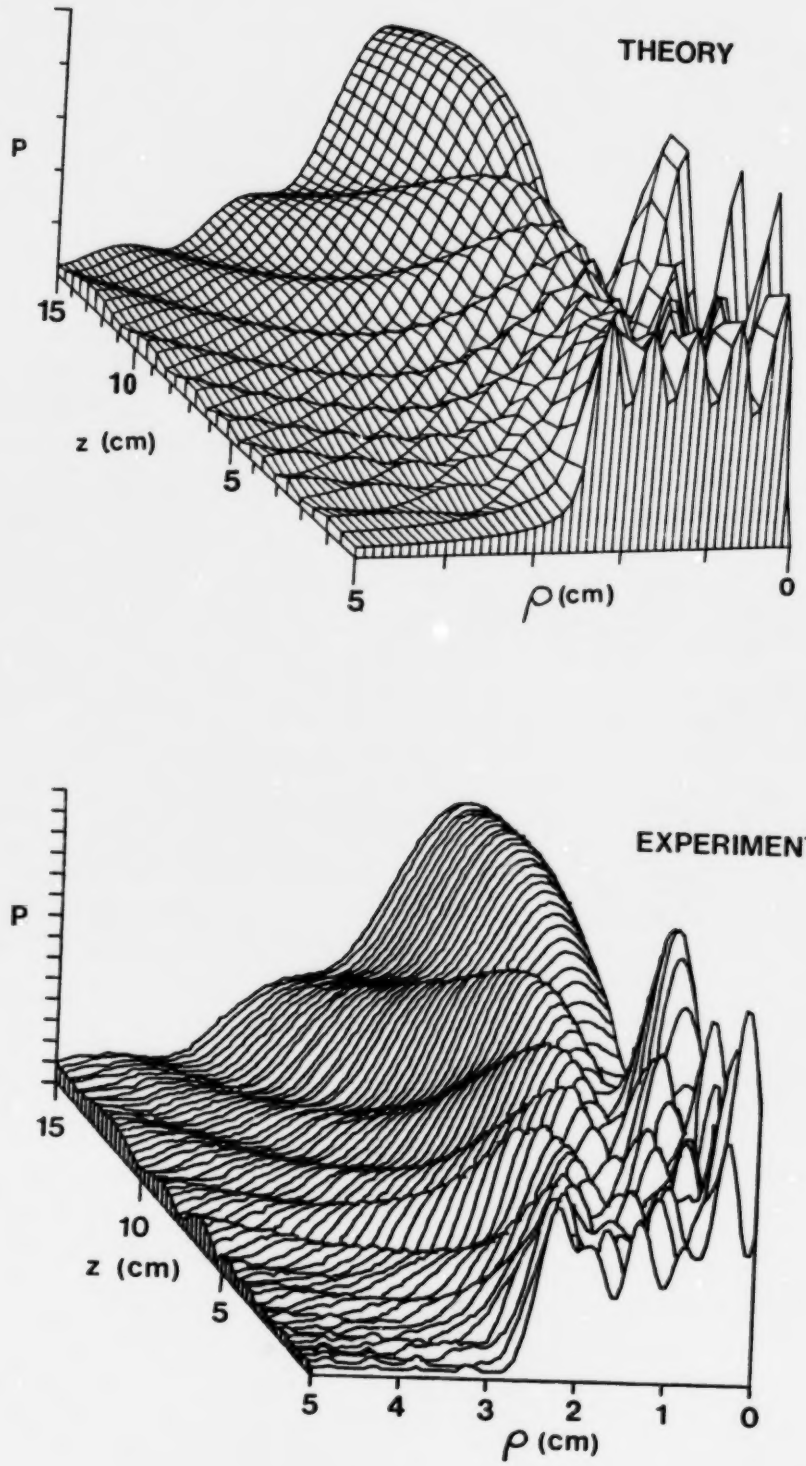

Fig. 7 Direct comparison of theory (Fig. 2(b)) and experiment (Fig. 6(a)) for the case of a plane piston.

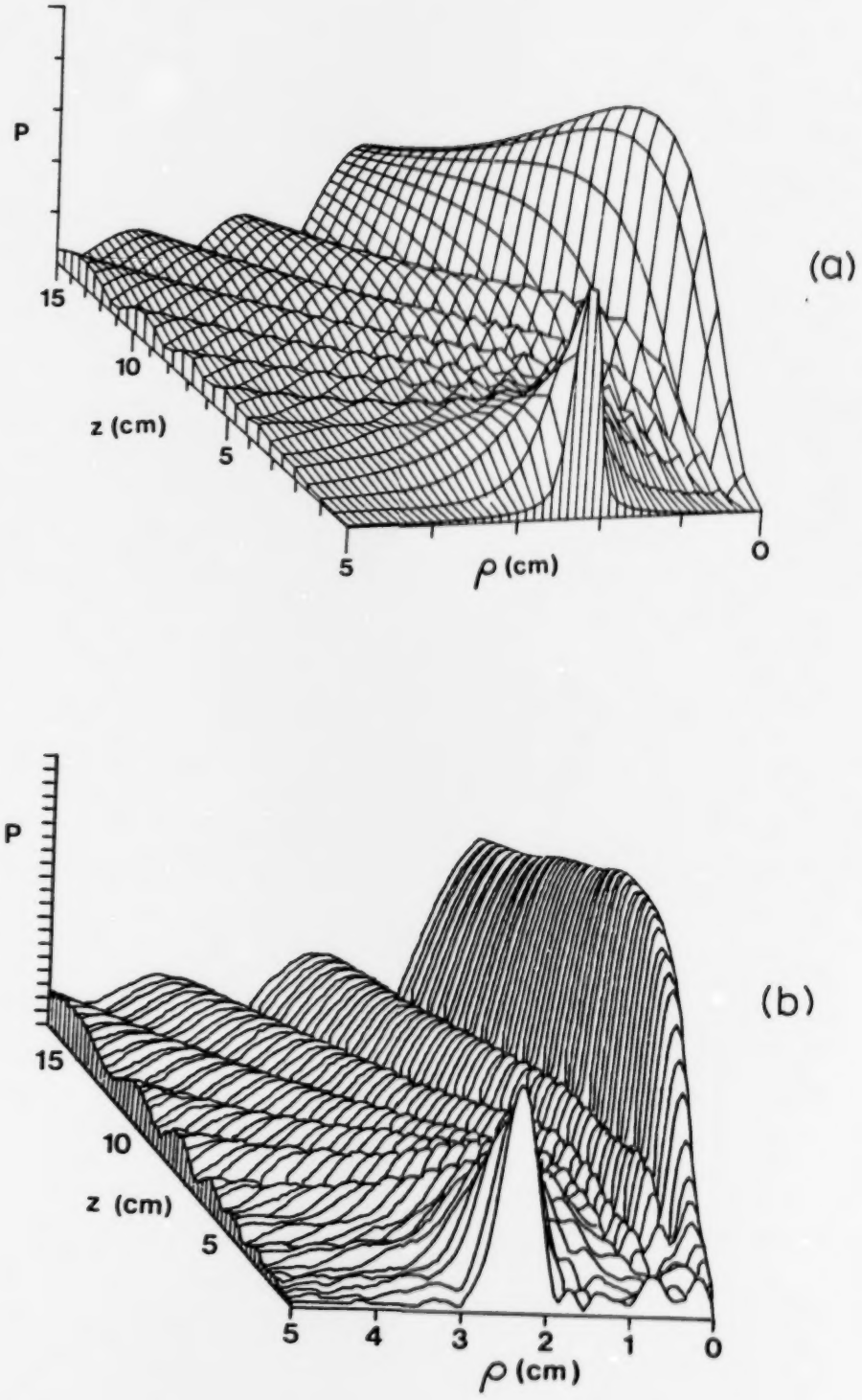

Fig. 8. Comparison of(a) theoretical and (b) experimental pressure fields for an annulus of outside radius 25mm and width 5mm. Theory assumed a uniform amplitude and phase over the face of the annulus, the experimental transducer being fabricated from PVDF. Frequency of excitation was 300kHz.

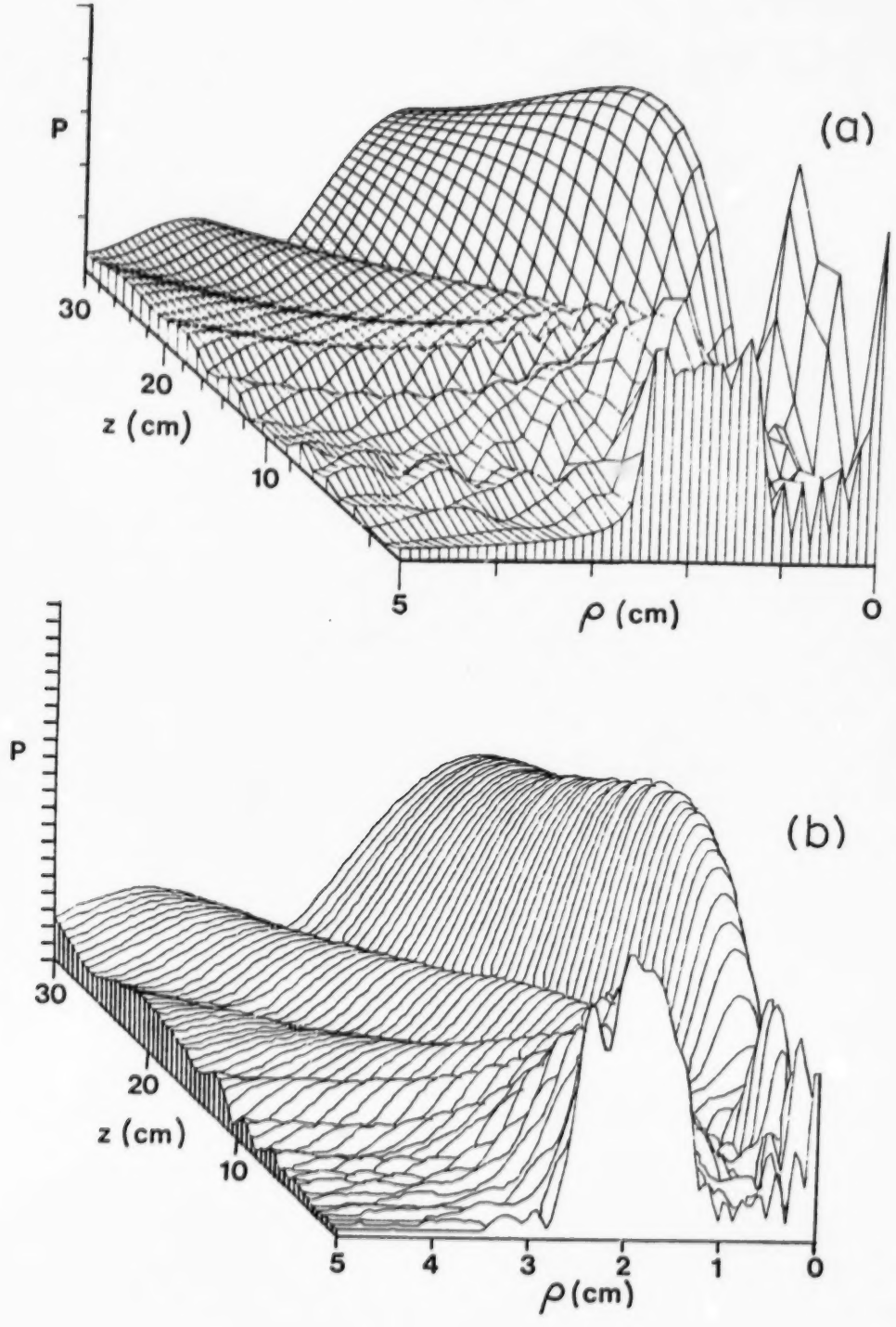

Fig. 9 Comparison of (a) theory and (b) experiment for a PVDF annulus, of outside diameter 50mm and width 25mm. Frequency of excitation was 400kHz.

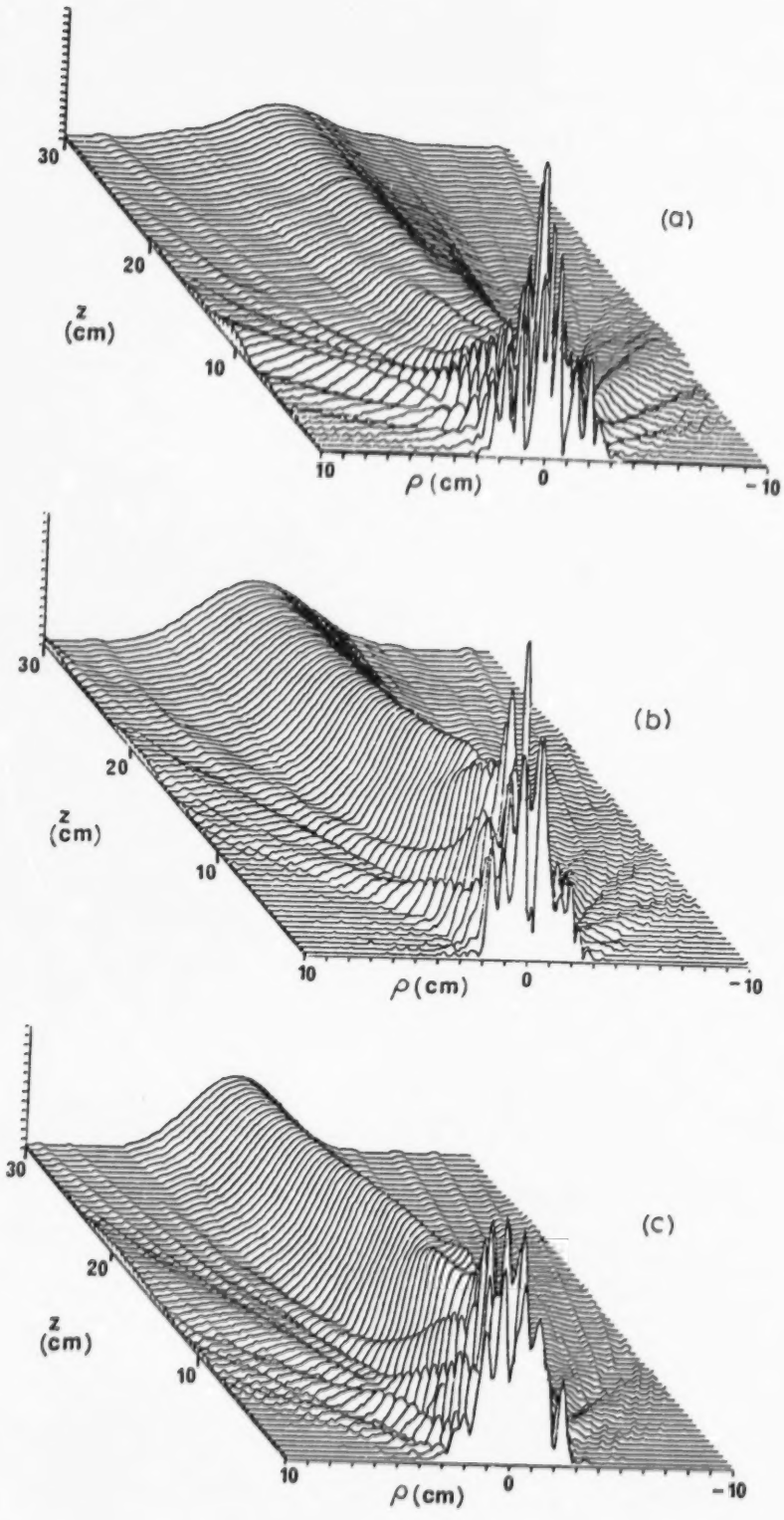

Fig. 10 Experimental pressure fields in water of a 50.8mm diameter PZT disc, excited at 293 kHz, (b) 300 kHz and (c) 304.2 kHz. Note axial symmetry in each of the fields.

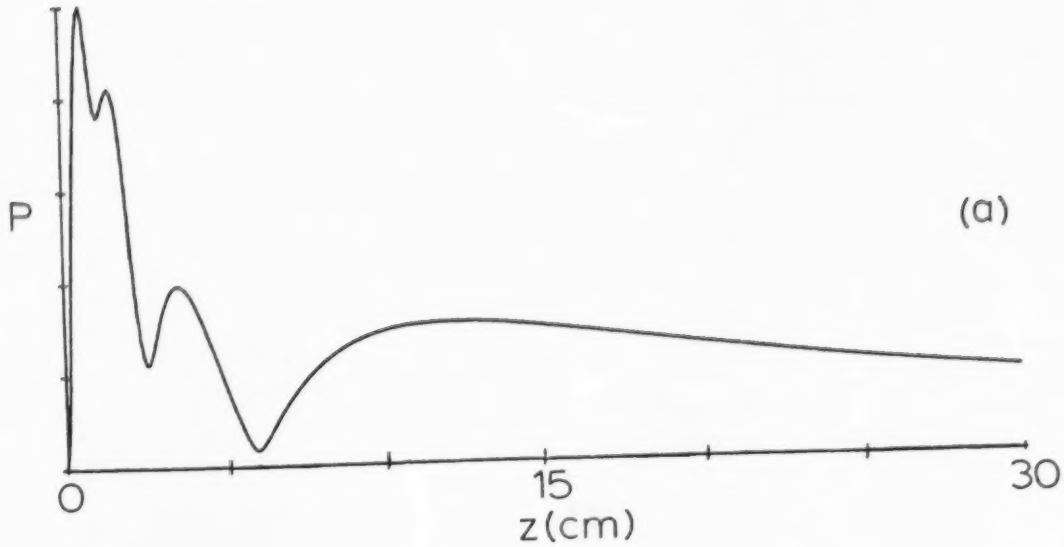

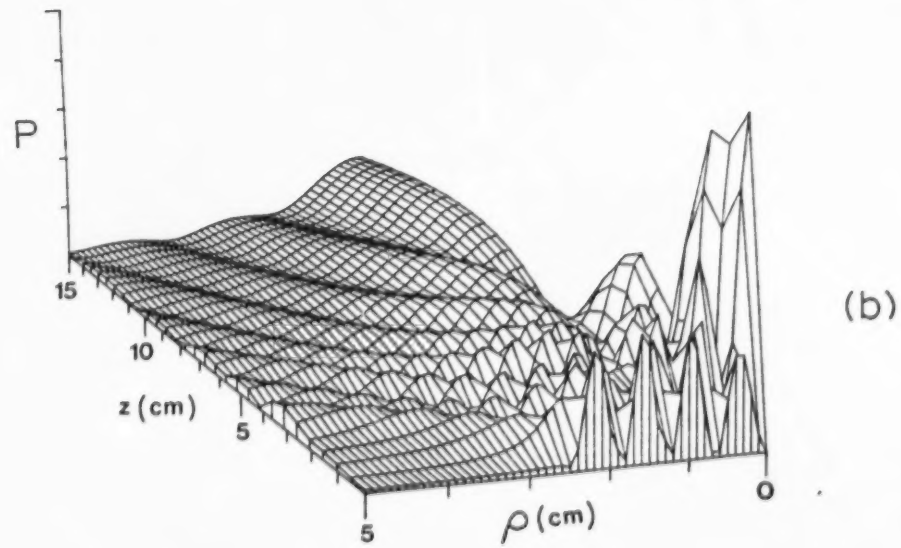

Fig. 11 Theoretical pressure field of disc, vibrating such that a=5λ, whose amplitude of particle velocity U_z varied as four cycles of a cosine function across its radius. (a) axial field, (b) three-dimensional distribution.

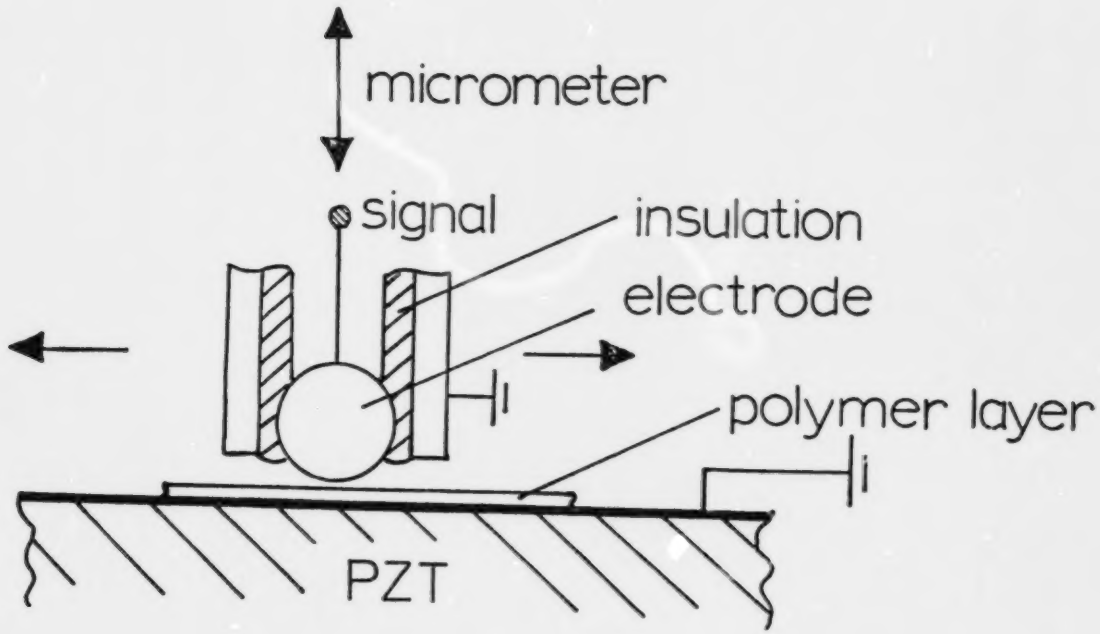

Fig. 12 Schematic diagram of ball-bearing type capacitance transducer, used to sample the displacements U_z normal to the transducer face.

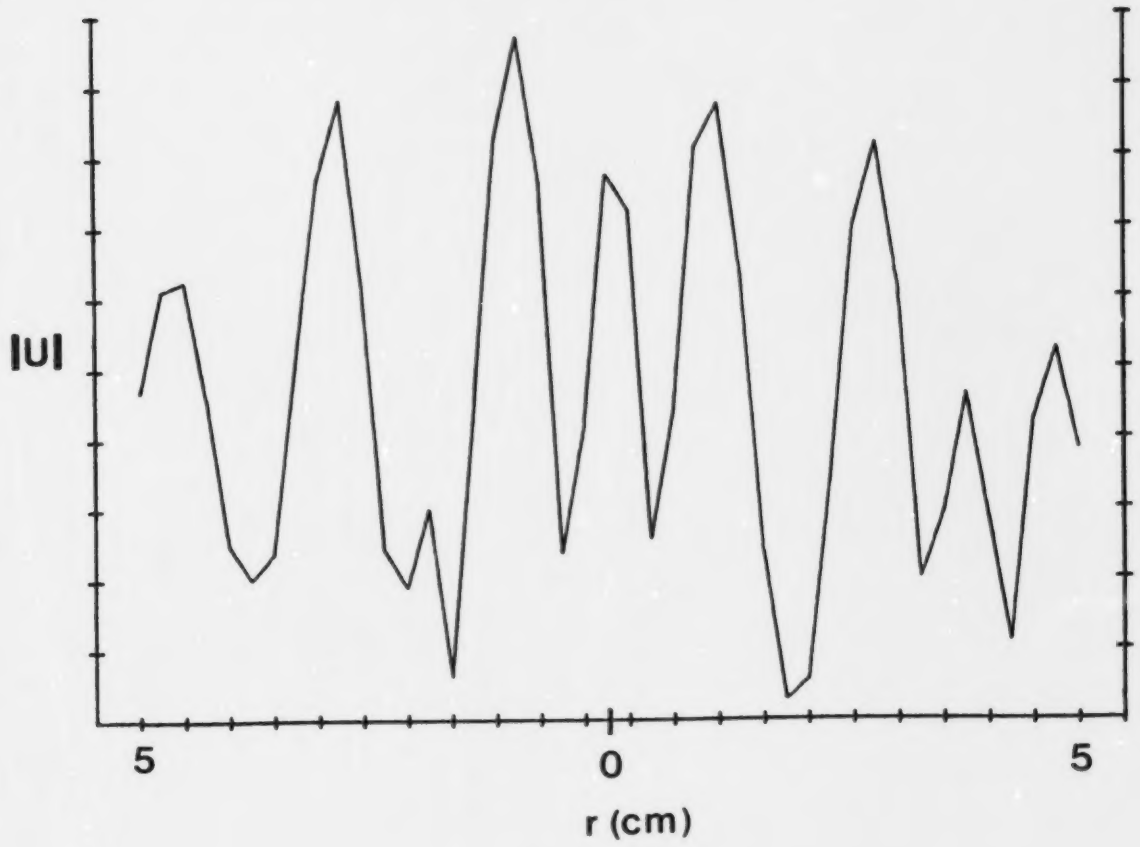

Fig. 13 The amplitude of displacements across the diameter of a 50.8mm disc, excited in air at 297 kHz.

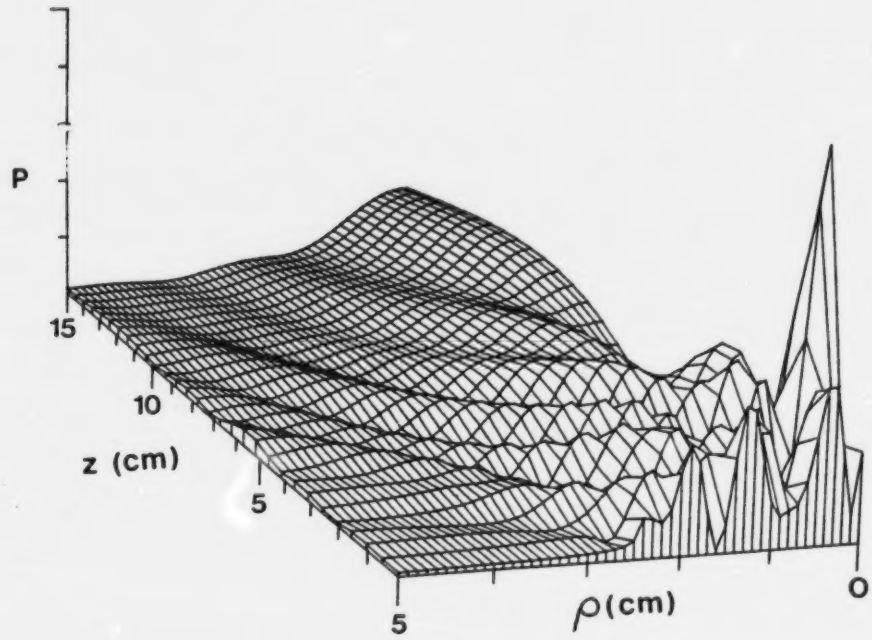

(a)

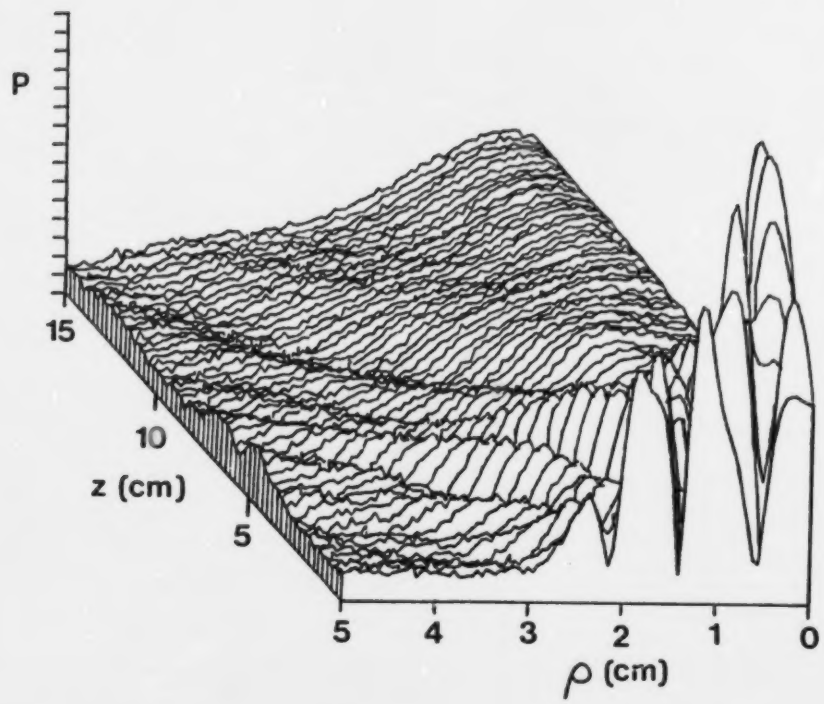

(b)

Fig. 14 (a) The pressure field predicted theoretically for a disc whose face is assumed to vibrate with the amplitude and phase variations of Fig. 13, compared directly to the experimental field at 293kHz (b).

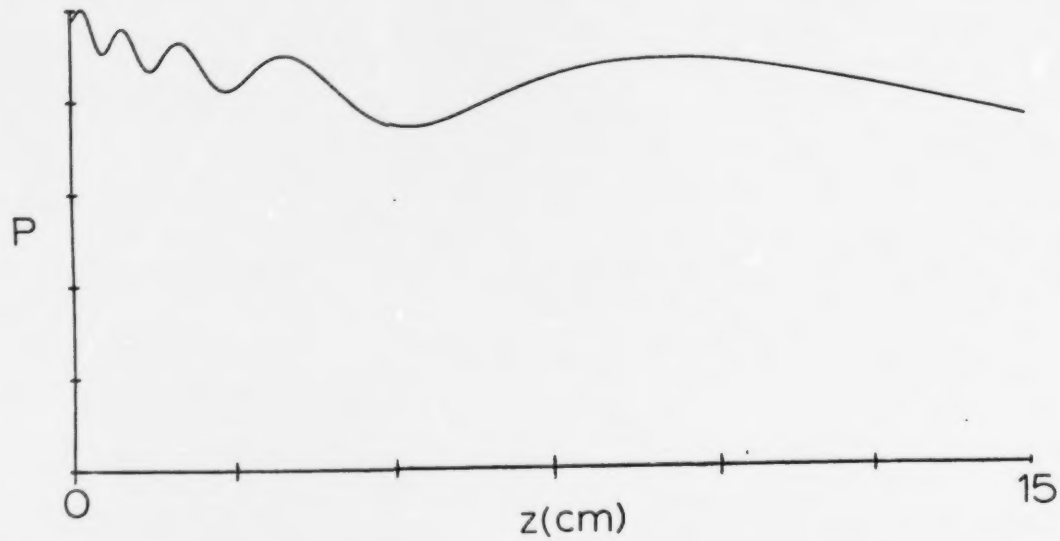

(a)

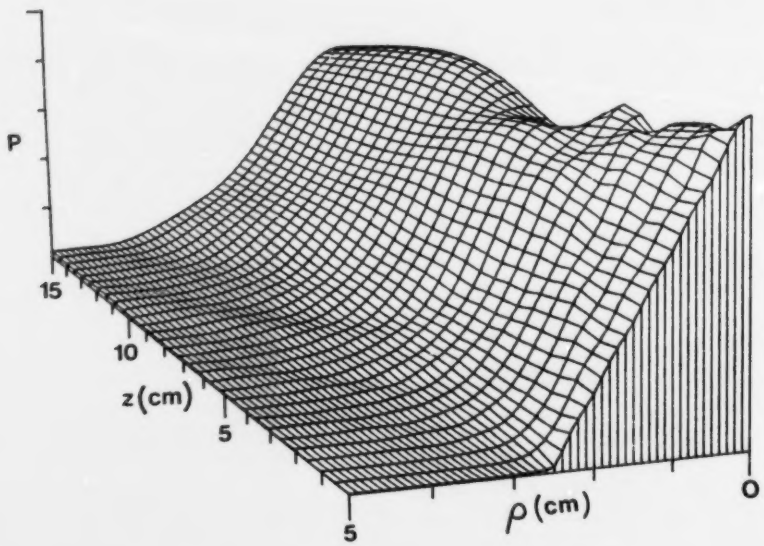

Fig. 15 Theoretical presure fields of discs whose amplitude of vibration U_z varies with radius (a) a linear decrease to zero at the disc edge; (b) constant amplitude over $0<\rho<4a/5$, and a linear decrease to zero at the disc edge thereafter; (c) a linear increase from zero at the disc edge to a maximum at its centre. $a=5\lambda$ throughout. Upper trace of each is the axial field, lower trace the three dimensional distribution.

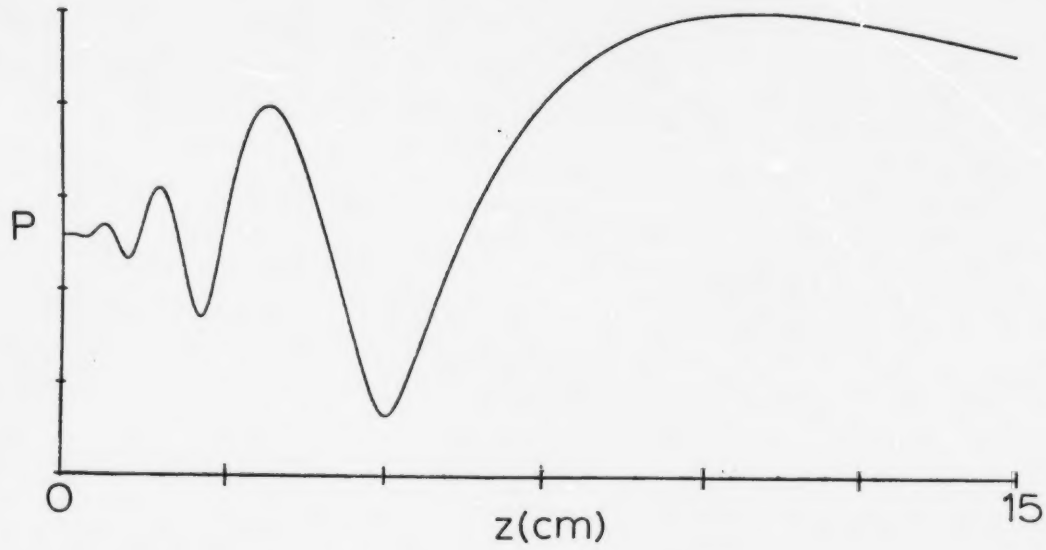

(b)

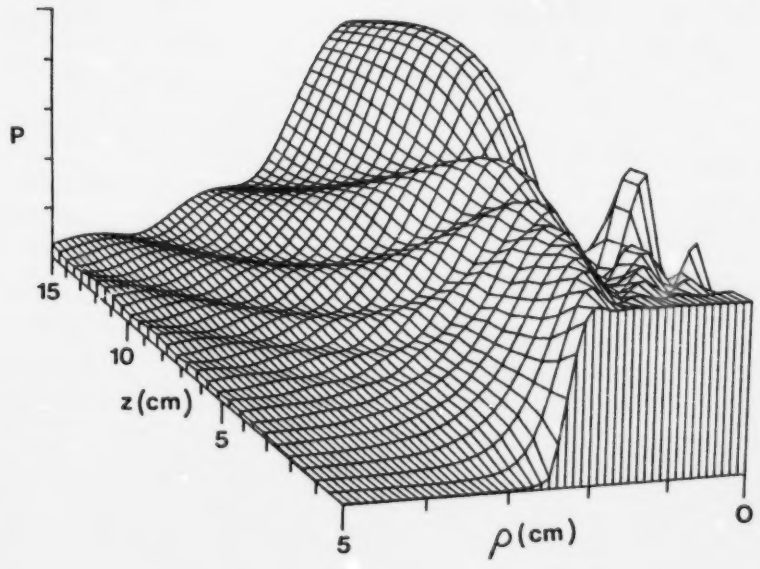

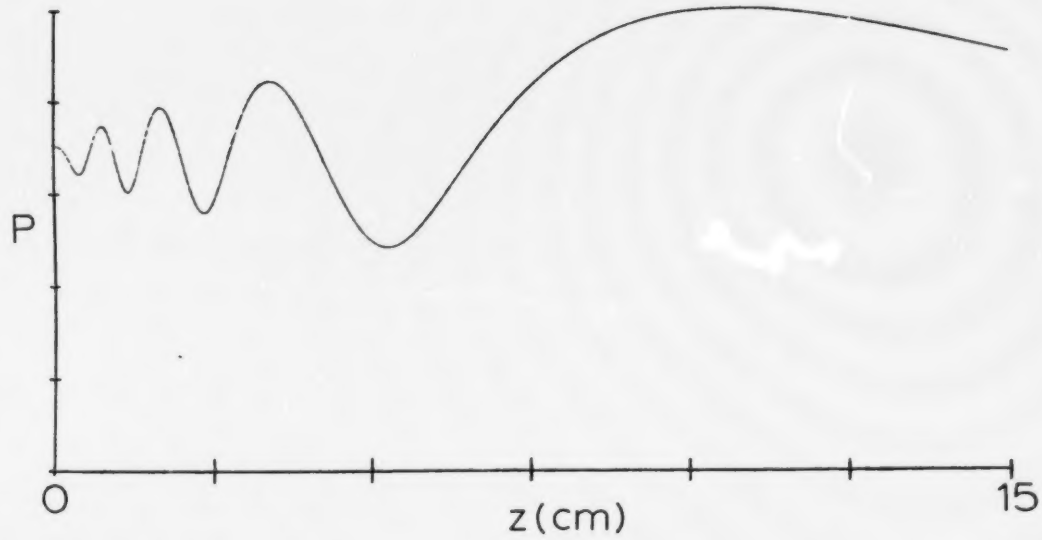

(c)

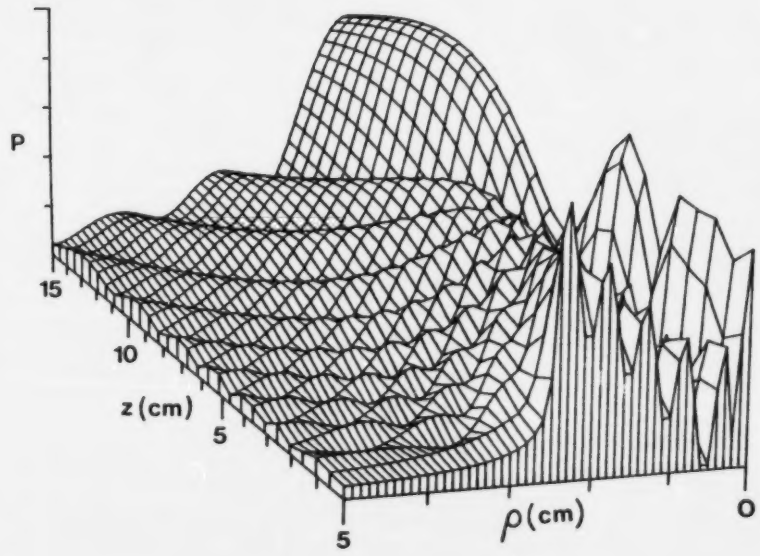

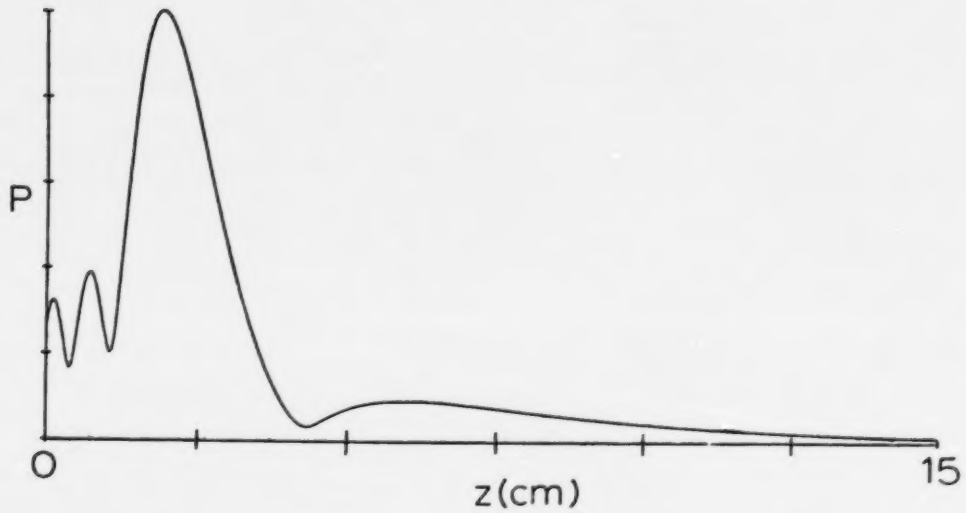

(a)

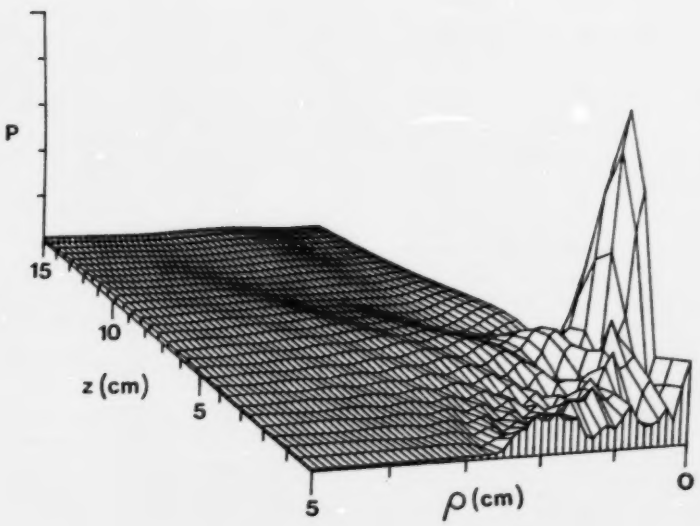

Fig. 16 Theoretical pressure fields of a disc radiator fabricated from two concentric annuli, surrounding a central disc. The phase of each component was constant across its width, but adjusted so that focusing would be expected to occur at (a) 2cm, (b) 5cm and (c) 10cm from the disc. Upper trace of each is the axial field, lower the three-dimensional distribution. a=25mm, disc vibrated at 300 kHz (a~5λ in water).

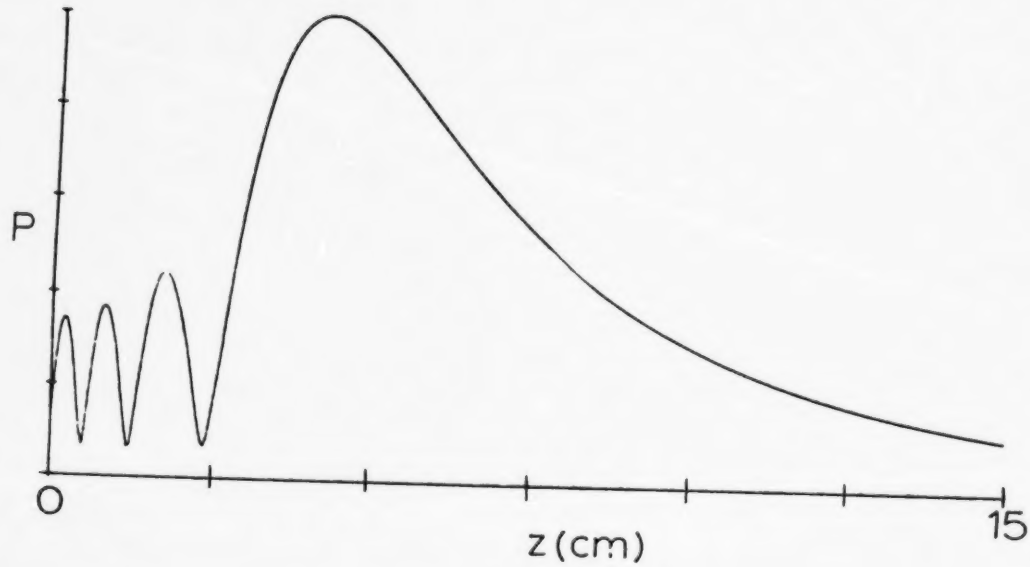

(b)

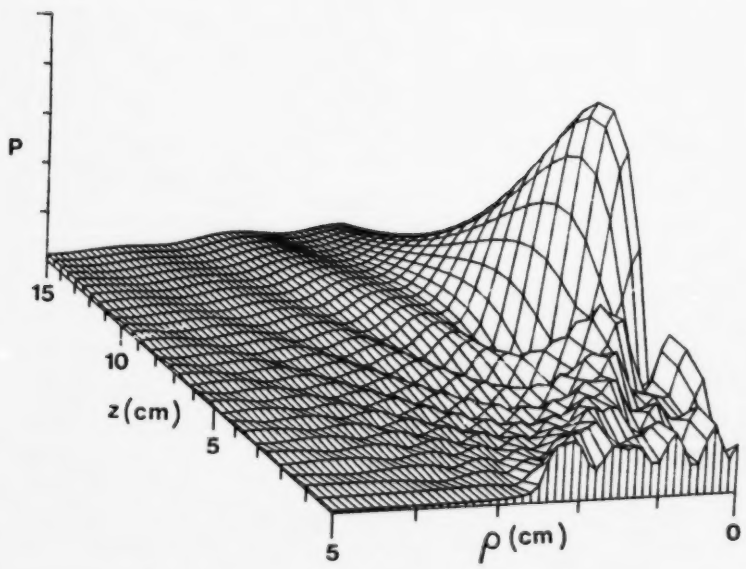

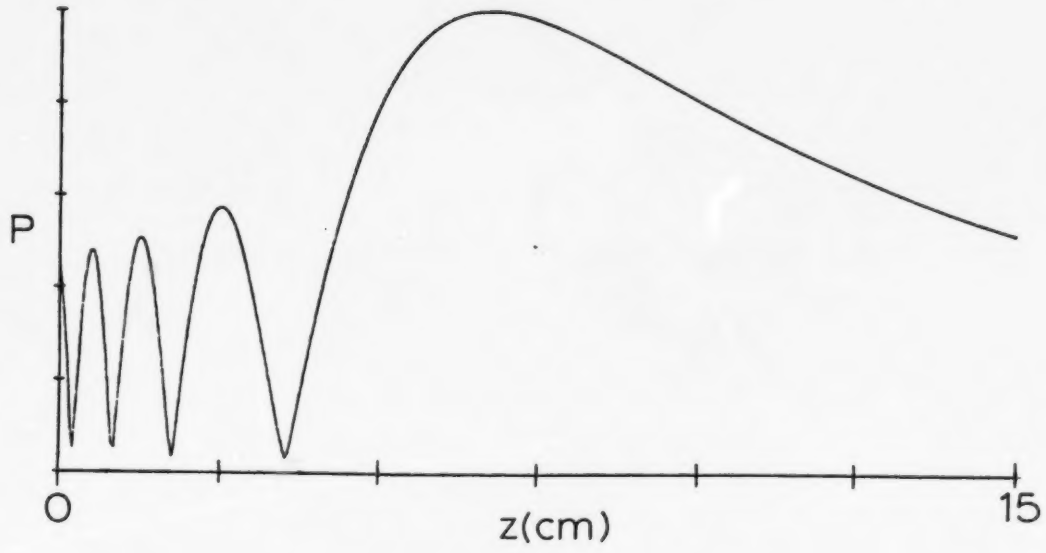

(C)

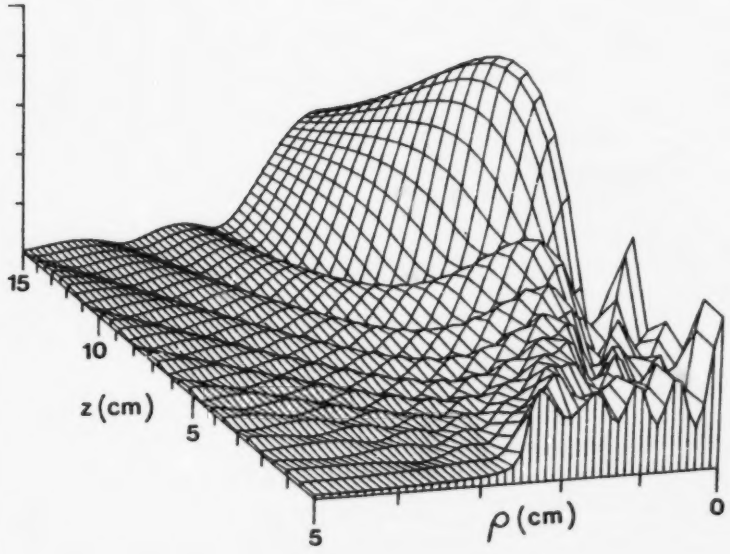

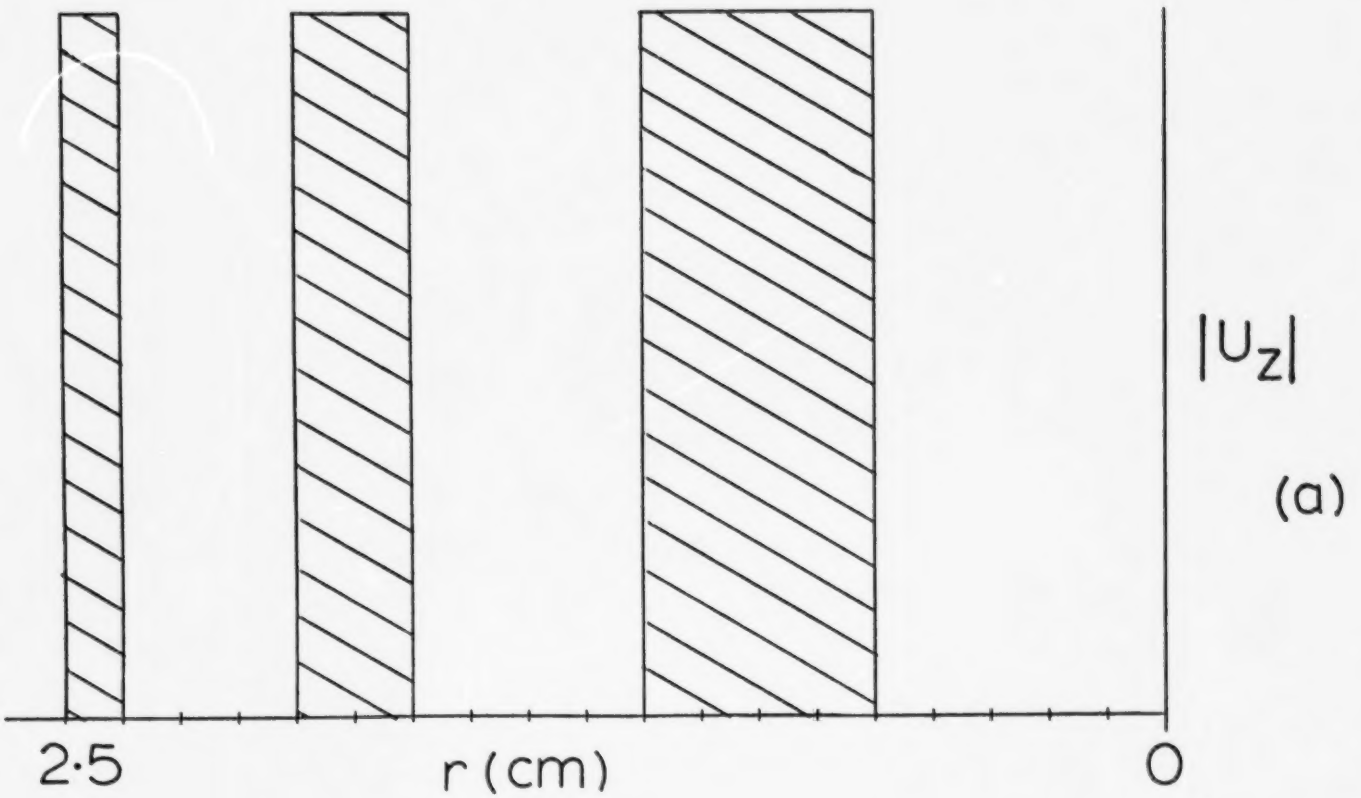

Fig. 17 Predicted theoretical field (b) of a Fresnel zone plate transducer, whose zones are as shown in (a). For excitation such that a=5λ, the expected focus would be on axis, at 20mm from the disc face of diameter 5cm.

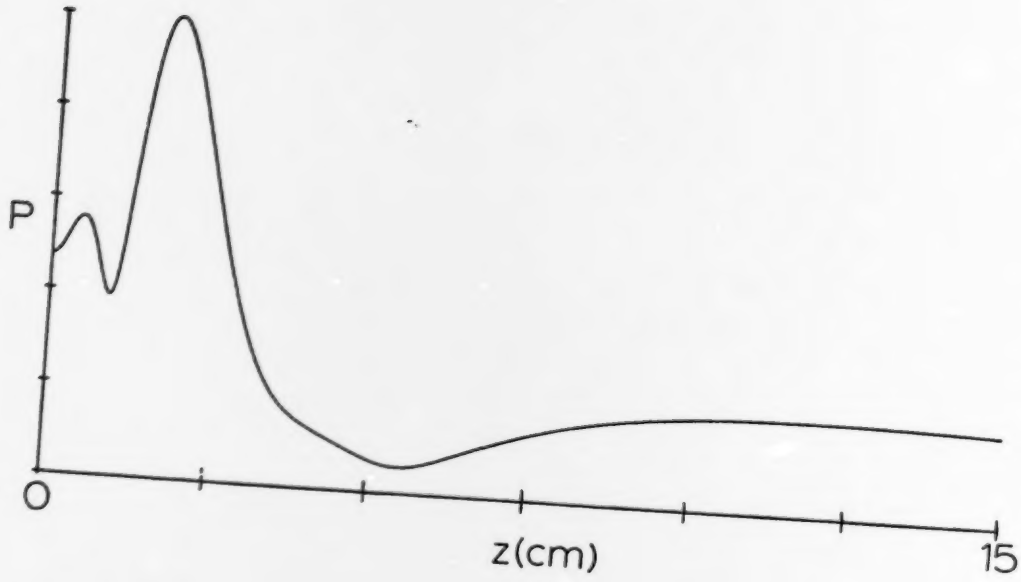

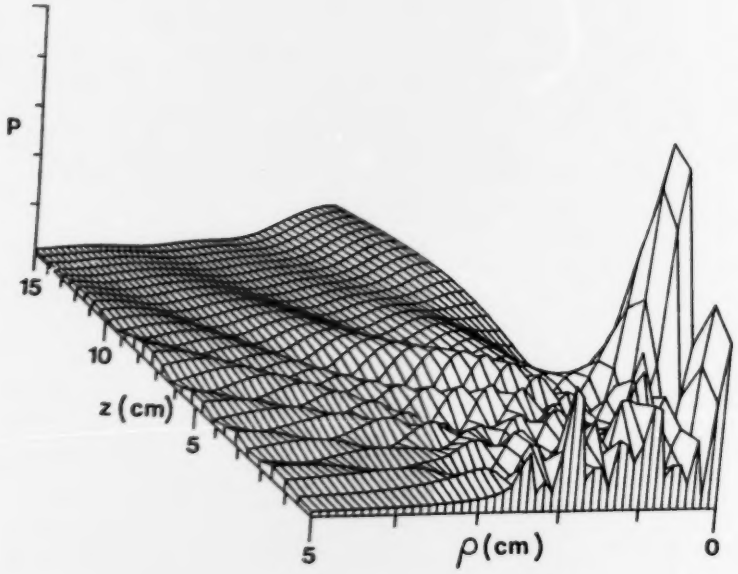

(b)